Deconvolution of activated and variable-range-hopping conduction for barely insulating arsenic-doped silicon

T. G. Castner and W. N. Shafarman*
University of Rochester, Rochester, New York 14627
(Received 19 March 1999)

An explanation, using the logarithmic derivative method, is given for some previously unexplained features of the temperature dependence of the conductivity for barely insulating Si:As for 10 K $<T<$ 78 K. The results and analysis suggest an important high-temperature correction to the prefactor of Mott variable range hopping, and also give more reliable values of the activation energy and the temperature-dependent prefactors of the activated conduction. The two samples closest to n_c provide evidence for temperature-dependent activation energies. The activated contribution allows the determination of the mobility $\mu(n,T)$ for itinerant electrons above the mobility edge. This mobility is consistent with ionized impurity scattering in the impurity band. The logarithmic derivative method also provides a method for determining the fraction $f_a(n,T)$ of donor electrons thermally excited above the mobility edge. The activated conductivity results are compared with Manfield's expression for impurity scattering as adapted to the impurity band case. [S0163-1829(99)06039-7]

I. INTRODUCTION

In the early period of semiconductor transport studies Fritzsche,[1] with resistivity measurements versus temperature, documented the activation energies ϵ_1, ϵ_2, and ϵ_3 from the slopes of $\ln \rho(T)$ versus $1/T$ plots. For n-type material ϵ_1 was the activation energy (from a donor or donor band) to the conduction band, ϵ_2 was the activation energy to the upper Hubbard band, while ϵ_3 was the activation energy for nearest-neighbor hopping when compensation was significant. The theory for the latter was provided by Miller and Abrahams[2] (MA). Then Mott[3] put forward the notion of variable range hopping (VRH) with a temperature-dependent activation energy. Allen and Adkins[4] first documented Mott VRH for Ge:Sb. The Mott formulation neglected the effect of electron-electron interactions, but Efros and Shklovskii[5] (ES) introduced VRH in the presence of interactions and a soft Coulomb gap in the density of states (DOS). There followed many experimental studies showing either Mott or ES VRH behavior and some studies showing a crossover between Mott VRH and ES VRH by varying magnetic field,[6] decreasing temperature,[7–9] and dopant density. Several theoretical formulations[10,11] have been given to describe the crossover. An early discussion of the crossover from ϵ_3 hopping to Mott VRH in the dilute limit has been given by Shklovskii.[12] Very close to the metal-insulator transition (MIT) on the insulating side, Shafarman, Koon, and Castner[13] (SKC) studied the critical behavior of Mott VRH for weakly compensated Si:As and found the Mott characteristic temperature T_0 $\{T_0 \propto [1/N(E_F)\xi^3]\}$ scaling to zero as $N_D \rightarrow n_{c-}$. A logarithmic derivative (LD) technique, first discussed by Hill,[14] was employed by SKC for the temperature range $0.6<T<78$ K. The results showed Mott VRH for $T<8$ K, activated hopping for $T>40$ K, and a broad negative slope region between the two that was not understood at the time. The present paper gives a detailed quantitative explanation for this intermediate regime where both activated and Mott VRH conduction are important. There have been few detailed studies of the crossover between Mott VRH and activated conduction, however, resistivity and Hall coefficient data[15] for insulating n-type CdSe have been obtained in the same temperature range. Zabrodskii and co-workers[16] have studied the crossover between ϵ_3 hopping and ES VRH in transmutation doped Ge:Ga with a compensation $K=0.3$ and have used the logarithmic derivative (LD) approach to obtain the T dependence of the activation energy. The results within illustrate how incorrect activation energies can be obtained from the slope of a $\ln \rho(T)$ versus $1/T$ plot. In addition, the LD approach can yield information on the T dependence of the prefactors of both activated and VRH conduction.

Derivative spectroscopy has been valuable in magnetic resonance in resolving partially overlapping resonance lines, while in tunneling studies[17] the derivative technique has been useful in yielding the density of states and features in the latter such as the $(E-E_F)^2$ dependence of the DOS within the Coulomb gap. It is not practical to modulate the temperature T by a constant amount because of specific heat variations with T and thermal time constants. However, even with the limitation of point-to-point data collection the LD technique, as pioneered by Moebius[18] and Moebius *et al.*,[19] has been valuable in MIT studies in determining whether a sample is metallic or insulating. They note for a metallic sample the LD $\delta(T)$ must approach zero as $T \rightarrow 0$, while for an insulating sample $\delta(T)$ must continually increase as $T \rightarrow 0$. Frequently, one cannot decide whether a sample is insulating or metallic on the basis of just the $\sigma(T)$ data. The application discussed here gives a more accurate way of determining activation energies, in addition to providing insight on VRH conduction at much higher temperatures than is possible with just the $\sigma(T)$ data. Simple theoretical notions suggest an important correction to the prefactor for Mott VRH and this correction factor also allows a direct determination of the mobility of activated itinerant electrons in the impurity band.

II. BACKGROUND

For barely insulating samples the Fermi level E_F is located in a region of localized states. The density of states for

 ©1999 The American Physical Society

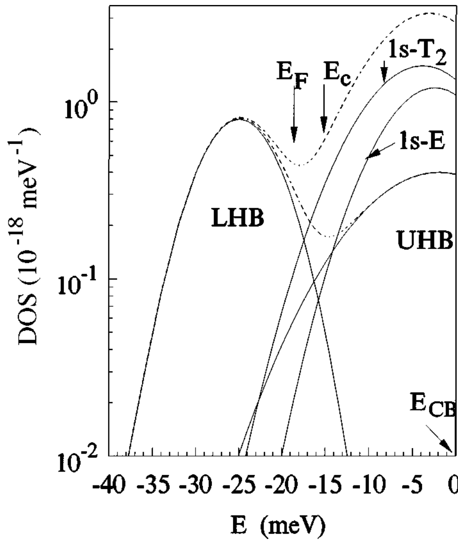

FIG. 1. The DOS $N(E)$ of the impurity bands for Gaussian bands for the LHB, the UHB, the $1s$-T_2 bands and the $1s$-E bands for $N_d=10^{18}/\mathrm{cm}^3$. The Gaussian widths are, respectively, 6, 12, 8, and 8 meV, while the peak positions are, respectively, at -25, -2, -3.9, and -2.5 meV based on the constancy of the valley-orbit matrix elements with donor density. The minimum in the total $N(E)$ of all four bands is at -17.6 meV while $E_F=\mu(0)=-18.1$ meV. If one removes the $1s$-T_2 and $1s$-E bands and considers the single-valley Hubbard band model $E_{\min}=-14.7$ meV and $E_F=-17.3$ meV.

Si:As based on both the conventional Hubbard model and the many-valley case characteristic of n-type Si is shown in Fig. 1. It shows the lower Hubbard band (LHB, $1s$-A_1-singly occupied), the upper Hubbard band (UHB, $1s$-A_1-doubly occupied), the $1s$-T_2 band (threefold orbital degeneracy), and the $1s$-E band (twofold orbital degeneracy). Gaussian shaped impurity bands have been employed, as utilized by Stern[20] in considering the screening length as $T\rightarrow 0$, as a reasonable approximation for impurity band shapes for a random distribution of donors. The positions of these hands, relative to the conduction-band edge E_{CB}, are based on spectroscopic data[21] and a self-consistent calculation[22] of $E_{1s\text{-}A1}(n,T=0)$ as n approaches n_c. For the specific case in Fig. 1 the maxima in the DOS for the individual bands are $E_{\mathrm{LHB}}=-25.0$ meV, $E_{\mathrm{UHB}}=-2.0$ meV, $E_{1s\text{-}T2}=-3.9$ meV, and $E_{1s\text{-}E}=-2.5$ meV. The valley-orbit splittings between the $1s$-A_1 and the $1s$-T_2 and $1s$-E states, which result from the very short-range, donor-dependent central cell potential, are not significantly affected by screening from e-e interactions at higher donor densities near n_c and are assumed the same as in the dilute limit. The band widths in Fig. 1 are $\Delta_{\mathrm{LHB}}=6.0$ meV, $\Delta_{1s\text{-}T2}=\Delta_{1s\text{-}E}=8.0$ meV, and $\Delta_{\mathrm{UHB}}=12.0$ meV and reflect the larger Bohr radii of the $1s$-T_2, $1s$-E, and UHB states that are much less tightly bound (with respect to E_{CB}) than the LHB. The energy $E_{1s\text{-}A1}(n)\sim-25$ meV, which corresponds to that expected for $n=0.86n_c$ based on results in Ref. 22. Reliable experimental values of $E_{\mathrm{CB}}-E_{1s\text{-}A1}(n)$ for Si:As for n just below n_c are not available. In Stern's case the width of the Gaussian band at low T arose solely from compensation and depended on the ionized acceptors (N_A^-) and ionized donors (N_D^+). For $N_D\sim 8\times 10^{18}/\mathrm{cm}^3$ and $K\sim 10^{-4}$ Stern's expression yields a width $\Delta\sim 1$ meV. The widths in Fig. 1 are much larger and result from the width of an impurity band for a regular array of neutral donors, plus some additional broadening from the randomness of the donor distribution.

The Fermi energy $E_F(T=0)$ is determined for the two-band case (LHB and UHB only) from the condition $\int_{EF}^{\infty}N_{\mathrm{LHB}}(E)dE=\int_{-\infty}^{EF}N_{\mathrm{UHB}}(E)dE$, namely, that the number of holes in the LHB equals the number of electrons in the UHB. This yields $E_F=-17.3$ meV and the minimum ($E_{\min}$) in the $\mathrm{DOS}_{\mathrm{total}}$ (lower dashed line) for this two-band case is at -14.7 meV. Adding the $1s$-T_2 and $1s$-E bands the RHS of the condition involves $N_{\mathrm{UHB}}(E)+N_{1s\text{-}T2}(E)+N_{1s\text{-}E}(E)$ and E_F is lowered to -18.1 meV, a decrease of 0.8 meV. The minimum in the $\mathrm{DOS}_{\mathrm{total}}$ (upper dashed line) for the many-valley case is at -17.6 meV, a decrease of 2.9 meV. In both cases $E_F<E_{\min}$ because the LHB width is smaller than that of the higher energy bands. In the relevant many-valley, four-band case $E_{\min}-E_F\sim 0.5$ meV, This value, compared with the larger experimental activation energies $E_a=E_c-E_F$ obtained for the four Si:As samples discussed herein, suggests that $E_c>E_{\min}$ so that E_c and E_F may lie on opposite sides of $E_{\min}$. Since $\epsilon_2=E_a(n)$ scales toward zero as $n\rightarrow n_{c-}$, both E_c and E_F are close to the minimum in the $\mathrm{DOS}_t(E)$, but E_F is much closer to $E_{\min}$ than E_c. For broader bands E_F can be above $E_{\min}$.

A weak random potential introduces localized states in the tails of an isolated band and produces two mobility edges for this band. However, for a sufficiently strong random potential all the states in this isolated band can be localized. In the case of strongly overlapping bands, as in Fig. 1, effectively there will be only a single mobility edge E_c, as indicated in Fig. 1 at an energy above $E_{\min}$. The position of $E_c(n,T\rightarrow 0)$ depends on the magnitude of the screened random potential (weak just below n_c) and is not accurately determined from calculations. While one might associate E_c with the lower mobility edge of the UHB, in the multivalley case with the $1s$-T_2 and $1s$-E bands strongly overlapping the UHB E_c should be identified with this complex of band states rather than with a single band. One should not expect different E_c's for the UHB, $1s$-T_2, and $1s$-E bands because this would lead to the coexistence of localized and itinerant states at the same energy. This is not expected to happen in single phase random systems except in unusual circumstances. Because the upper mobility edge associated with the LHB must be well below E_F in energy, it will play no role in T-dependent transport at relatively low T.

The fact that both E_F and E_c are relatively close to $E_{\min}$ for the total DOS has important implications for the transport, namely, for the activated conduction and for the VRH conduction of the Mott form. It is the total DOS of the LHB, the UHB, and the $1s$-T_2 and $1s$-E bands that is important for the VRH. This can be seen because the LHB consists of singly occupied donor states while the UHB consists of doubly occupied states. An electron in the LHB can be excited to a state in the UHB, or to the $1s$-T_2 or $1s$-E bands, or to a empty state (hole) in the LHB. The same is true of the excitation of occupied states in the UHB or the $1s$-T_2 and $1s$-E bands. Thus, it is not the single Hubbard band DOS that is important for the Mott VRH, but it is the total DOS from all

the overlapping bands that enters Mott's formulation of VRH.

The minimum in DOS_{total} is shallower than for the simple Hubbard band case with just LHB and UHB and this has implications for the T dependence of the chemical potential $\mu(T)$. Finally, the shape of $DOS_{total}(E)$ in Fig. 1 can be significantly altered for the many-valley case by changing the widths of the $1s$-T_2 and $1s$-E bands. If these bands are broadened by 25% relative to those shown in Fig. 1 the minimum in $DOS_{total}(E)$ will disappear and be replaced by an inflection point. However, even in this case the total DOS is slowly varying in the immediate vicinity of the inflection point.

For barely insulating samples the temperature-dependent conductivity $\sigma(T)$ consists of two types of contributions, namely, a hopping contribution $\sigma_h(T)$ for transitions between localized states and an activated contribution $\sigma_a(T)$ resulting from thermal excitation of electrons into extended states with energies above the mobility edge E_c. For the latter the thermal activation is to states with $E_c<E<E_{CB}$ in the impurity conduction band. The impurity band conduction is characterized by an activation energy $\epsilon_2=E_c-\mu(T)=E_a$. Thermal activation to states with $E>E_{CB}$ [with activation energy $\epsilon_1(n)$] can also occur, but will represent a negligibly small fraction of $\sigma_a(T)$ because $\epsilon_1(n)$ is considerably larger than $\epsilon_2(n)$ as n approaches n_c. $\sigma_a(T)$ results from itinerant electrons in extended states above E_c in the impurity band. These itinerant electrons have a mobility that is similar to itinerant electrons in the host Si CB. The activation energy $\epsilon_3(n)$ from Ref. 1 is associated with nearest-neighbor hopping between localized states and results from compensation. This contribution is negligible for n just below n_c for weakly compensated samples ($N_A/N_D \ll 1$, where N_D and N_A are the donor and acceptor concentrations). The hopping considered below is Mott VRH because the hopping energy $\Delta_h(T)$ is greater than the Coulomb gap width associated with ES VRH. This is the case for Si:As and Si:P for $1\text{-}n/n_c<0.1$.

For the data analysis the VRH contribution is taken as $\ln\sigma_h(T)=\ln[A(n)(1/T)^s]-(T_0/T)^m$ where $m\sim 1/4$ for Mott VRH, $A(n)$ is a density-dependent constant, and $s(n)$ is the exponent for the prefactor T dependence. The activated term is of the form $\sigma_a=\Sigma\sigma_{0,i}(T)^{p,i}e^{-Ei(T)/kT}$ where E_i is the activation energy for the ith activation process and p_i is the power-law exponent of the prefactor. Below only a single component of activated conduction will be considered in the data analysis, but the analysis is readily generalized to multiple components with different E_i. Defining the logarithmic derivative (LD) $\delta=-d\ln\sigma(T)/d\ln(1/T)$ one obtains

$$\delta_a=-d\ln\sigma_a/d\ln(1/T)=p+E_a(T)/kT-dE_a/dkT, \quad (1a)$$

$$\delta_h=-d\ln\sigma_h/d\ln(1/T)=-s+m(T_o/T)^m. \quad (1b)$$

The third term on the right of Eq. (1a) results from a temperature-dependent activation energy and is related to the changes in the chemical potential $\delta\mu(T)$ and $E_c(T)$. With $E_a(T)=E_c-\mu(T)$, where the Fermi energy at $T=0$ is $\mu(0)=E_F$, $dE_a/dT=dE_c/dT-d\mu/dT$ and $\delta_a=p+E_a(0)/T+(T/)[d(\mu/T)/dT]$, where we have set $k=1$ and measure T in energy units. The temperature dependence of $\mu(T)$ is discussed in Sec. III. The second term in δ_h in Eq. (1b) can also be written as Δ_h/T, where $\Delta_h=1/4(T^3T_0)^{1/4}$ is the mean hopping energy. Qualitatively, both δ_a and δ_h increase with increasing values of $1/T$, although the latter increases at a slower rate since $m=1/4$ for Mott VRH. The total conductivity $\sigma_t(T)=\sigma_a(T)+\sigma_h(T)$ yields a total LD δ_t given by

$$\delta_t=(\sigma_a/\sigma_t)\delta_a+(\sigma_h/\sigma_t)\delta_h. \quad (2)$$

The Mott VRH expression $\ln\sigma_h=\ln[A(1/T)^s]-(T_0/T)^{1/4}$ is established by the data at sufficiently low temperatures where $\sigma_a \ll \sigma_h$ and $\sigma_t \sim \sigma_h$. At higher temperatures where σ_a is comparable to σ_h an increasingly larger fraction $f_a(n,T)$ of electrons are thermally excited above the mobility edge at E_c. This in turn implies only $(1\text{-}f_a)n$ of the electrons will be available for VRH conduction and suggests an important high-temperature correction to the prefactor of Mott VRH. One can calculate f_a using $n_h(T)+n_a(T)=n$, $f_a=n_a/n$, and the standard result

$$n_a=\int_{Ec}^{\infty}N(E)f(E,T)dE, \quad (3)$$

where $N(E)$ is the DOS and $f(E,T)$ is the Fermi function $f=[e^{(E-\mu(T))/T}+1]^{-1}$ with $\mu(T)$ the chemical potential. The activated contribution $\sigma_a=n_a(T)e\mu_a(T)=nef_a(T)\mu_a(T)$ where $\mu_a(T)$ is the mobility of activated carriers in extended states in the impurity conduction band. $\mu_a(T)$ is analogous to to the classical mobility of carriers in the CB $[E>E_{CB}]$ and will be determined by ionized impurity scattering in the n and T range of relevance.

For a constant $N(E)$ for $E>E_c$ one obtains $n_a=N(E_c)T\ln[1+e^{-Ea(n,T)/T}]$. If the DOS is expanded about $E_c[N(E)=N(E_c)+(dN/dE)_{Ec}(E-E_c)+\cdots]$ the next term in the expansion for n_a will be given approximately by $(dN/dE)_{Ec}T^2\ln[1+e^{-Ea/T}]$. Adding this term $n_a=N(E_c)T[1+\alpha T]\ln[1+y]$ where $\alpha(T)=d\ln N(E)/dE|_{Ec(T)}$ and $y=e^{-Ea/T}$. The experimental results and the DOS in Fig. 1 both suggest that $(dN/dE)_{Ec}T \ll N(E_c)$ in the low-T region. Based on the values of $E_a(n,T)$ and the $\mu(T)$ results in Fig. 2 it appears the DOS itself depends on T for $T>15$ K. However, it is difficult to incorporate the effects of a T-dependent DOS on f_a and an empirical form $f_{a,\text{emp}}(n,T)=BT^q\ln[1+e^{-(Ec-\mu(T))/T}]$ has been employed in the data analysis. B and q, which are coupled, are determined from the data near 77 K using the expression $f_a=\sigma_a/ne\mu_a(T)$. With $\sigma_{h,c}=\sigma_h(1-f_a)$ and $\sigma_{a,c}=\sigma_t-\sigma_{h,c}$ the corrected LD values $\delta_{h,c}$ and $\delta_{a,c}$ become

$$\delta_{h,c}=\delta_h-[f_a/(1-f_a)]d\ln f_a/d\ln T, \quad (4a)$$

$$\delta_{a,c}=(1/\sigma_{a,c})[\sigma_t\delta_t-\sigma_h(1-f_a)(\delta_{h,c})]. \quad (4b)$$

Using the result $\delta_{a,c}\equiv d\ln\sigma_{a,c}/d\ln T=d\ln f_a/d\ln T+d\ln\mu_{a,c}/d\ln T$ to eliminate $d\ln f_a/d\ln T$ from Eq. (4a) and substituting Eq. (4a) into Eq. (4b) one obtains the important result

$$\delta_{a,c}=\delta_a+[f_a\sigma_h/(\sigma_t-\sigma_h)][\delta_h-d\ln\mu_{a,c}/d\ln T]. \quad (5)$$

This exact result is useful since it allows a determination of $\delta_{a,c}$ if $f_a(T)$ is known since f_a determines $\sigma_{a,c}$, $\mu_{a,c}$, and $d\ln\mu_{a,c}/d\ln T$. However, this expression can also be used in an iterative manner to calculate $f_a(T)$ using $\delta_{a,c}$ values determined initially from $f_{a,\mathrm{emp}}$. The expression for $f_a(n,T)$ from Eq. (5) does not depend on the magnitude of $\mu_{a,c}(n,T)$. Arbitrary forms of $f_a(T)$ won't satisfy Eq. (5) and the requirement $0<f_a<1$. For example, if $f_a\propto T^n$ and $\sigma_{a,c}\propto T^m (m<n)$ one finds from Eq. (5) $f_a=[(\sigma_t-\sigma_h)/\sigma_h][(m-\delta_a)/(\delta_h+n-m)]$. f_a changes sign for $m<3-5$ since $\delta_a(T)$ increases with $1/T$ as shown in Fig. 6. Only a form $f_a\propto T^q e^{-Ea/T}$ $[d\ln f_a/d\ln T=q+E_a/T-dE_a/dT]$ gives a result that can explain the data. The condition $0<f_a<1$ and the data also restricts the values of $d\ln\mu_{a,c}/d\ln T$. For sample 8.41 $[n=0.98n_c]$ $-d\ln\mu_{a,c}/d\ln T>0.4$ for $T>60$ K to keep $f_a<1$ because of the small values of δ_h. The q in the empirical expression can depend on T and the series expansion approach suggests $q(T)=1+\eta(T)$ where $\eta(T)=\ln(1+\alpha T)/\ln(T/T_k)$ where T_k is a constant such that $T_k\ll T$. This expression for $\eta(T)$ neglects higher terms in the expansion. In the intermediate T regime the quantities σ_t and δ_t are measured, σ_h and δ_h are extrapolated from the lower-T region where Mott VRH dominates, and $d\ln\mu_{a,c}/d\ln T$ is inferred from the data. Using the expression $f_a(n,T)=N(E_c,T)kT(T/T_k)^{\eta}[\ln(1+e^{-Ea(n,T)/T})]$ one finds

$$d\ln f_a/d\ln T=[1+(E_a/T)\phi(y)]-\phi(y)dE_a/dT+d\ln N(E_c(T),T)/d\ln T+\ln(T/T_k)d\eta/d\ln T. \quad (6)$$

$E_a(n,T)$ is determined from the data (Fig. 5) and it also determines $\phi(y)=y/\{(1+y)\ln(1+y)\}$. The experimental results suggest $q\geq 1$. The second and third terms are harder to characterize, but with $dE_a/dT=dE_c/dT-d\mu/dT$ this suggests a coupling between these two terms. The last term is positive and of order $\alpha T/(1+\alpha T)$ where $\alpha(T)=d\ln N(E)/dE|_{Ec(T)}$. This term is very small at low T compared to the first term, but might be important at higher T. Using $d\ln N(E_c)/d\ln T=T/N(E_c)|dN(E)/dE|_{Ec}(dE_c/dT)=\alpha T(dE_c/dT)$, and $dE_c/dT=dE_a/dT+d\mu/dT$, $\delta_{a,c}$ becomes

$$\delta_{a,c}=1+E_a/T-dE_a/dT+\alpha T[dE_a/dT+d\mu/dT+(1+\alpha T)^{-1}]+d\ln N(E_c,T)/d\ln T+d\ln\mu_{a,c}/d\ln T. \quad (7)$$

The $\phi(y)$ term is dropped in Eq. (7) when the data is fit to $\sigma_{a,c}\propto e^{-Ea/T}$ rather than to $\ln[1+e^{-Ea/T}]$. For a T independent $N(E)$ if $d\mu/dT<0$ and $\mu(T)$ decreases more rapidly than the increase in $E_a(T)$ then $E_c(T)$ will decrease causing $N(E_c)$ [and also $\alpha(T)$] to decrease since $E_c(0)$ is well above $E_{\min}$. On the other hand, if $\mu(T)$ increases (unlikely for $T>20$ K) [or $\mu(T)\sim$const] while $E_a(T)$ increases with T then $E_c(T)$ increases and $d\ln N(E_c)/d\ln T>0$. For a T dependent $N(E,T)$ likely at higher T the situation is more complex, but leads to a nonzero $d\ln N(E_c)/d\ln T$. The parameter $\alpha(T)$, which is the fractional slope of $N(E)$ at E_c plays a key role in the higher order corrections for $\delta_{a,c}$. For the DOS in Fig. 1 one finds $\alpha=0.25$/meV for $E_a\sim 4$ meV. Thus, αT might be of order unity in the middle of our T range suggesting the corrections might be important. However, for αT near unity the dE_a/dT terms will nearly cancel. In addition, $d\mu/dT$ and $(1+\alpha T)^{-1}$ are of opposite sign above 20 K. Furthermore, if $E_c(T)$ approaches $E_{\min}$ at higher $T,\alpha(T)$ becomes small and these corrections become small. At lower T the fourth term in Eq. (7) will decrease as T leaving the third term as the correction. It is only the first three terms and the last term that are known from the experimental results. Hence, $\delta_{a,c}$ is calculated as $d\ln\sigma_{a,c}/d\ln T$ and then one attempts to infer the magnitude of the corrections.

III. TEMPERATURE DEPENDENCE OF THE CHEMICAL POTENTIAL $\mu(T)$

Of importance for determining the activation energy $E_c-\mu(T)$ appearing in $f_a(T)$ is the temperature dependence of $\mu(T)$. The classical semiconductor result[23] for the weak compensation, valid for $C_eT^{3/2}\gg N_A[C_e=2(2\pi m^*k/h^2)^{3/2}=6\times 10^{15}/\mathrm{cm}^3-\mathrm{K}^{3/2}$ for Si], is given by

$$\mu(T)=(E_{CB}+E_D)/2+T/2\ln[(N_D-N_A)/2C_eT^{3/2}]. \quad (8)$$

Equation (8) is based on discrete donor levels and therefore ignores impurity banding. It also neglects the contributions from the $1s$-T_2 and $1s$-E states. It yields a positive correction for $2C_eT^{3/2}<(N_D-N_A)$ and a negative correction for $2C_eT^{3/2}>(N_D-N_A)$. For Si:As with $N_D\sim 8\times 10^{18}/\mathrm{cm}^3$ and $N_A\ll N_D$ the crossover occurs at $T\sim 76$ K while at 40 K the correction is $\delta\mu=+1.6$ meV. The classical result is not relevant for the band situation shown in Fig. 1. Using $n_a(T)$ from Eq. (3) and the density of localized electrons $n_h=\int_{-\infty}^{Ec}N(E)f(E,T)dE$ involved in hopping, and the conservation condition $d/dT[n_a(T)+n_h(T)]=0$ it is straightforward to obtain

$$Td\mu/dT=-\int_{-\infty}^{\infty}(E-\mu)N(E)f(1-f)dE \Big/ \int_{-\infty}^{\infty}N(E)f(1-f)dE. \quad (9)$$

Using $f(1-f)=-(\partial f/\partial E)T$ and that $\partial f/\mathrm{E})$ is sharply peaked about $\mu(T)$, Eq. (9) can be evaluated by the Sommerfeld expansion approach (Appendix A). Alternatively, a direct numerical integration of the integrals in Eq. (9) can be performed at a series of equally spaced T.

Figure 2 shows the results for $\mu(T)$ for the total DOS $N(E)$ shown in Fig. 1 using parameters appropriate for Si:As for N_D just below n_c. Also shown is the classical dependence of $\mu(T)$ based on Eq. (8). This result, which neglects the $1s$-T_2 and $1s$-E states, shows a large positive increase that peaks for $T\sim 30$ K and then steadily decreases. The correction $\delta\mu(T)$ does not become negative until $T>80$ K. The negative decrease results from the conduction-band states with $E>E_{\mathrm{CB}}=0$. The band case (●), calculated with Eq. (9) using the integrals, exhibits a very shallow maximum and $\Delta\mu(T)$ turns negative for $T\sim 19$ K. For $T>50$ K $\mu(T)$ is

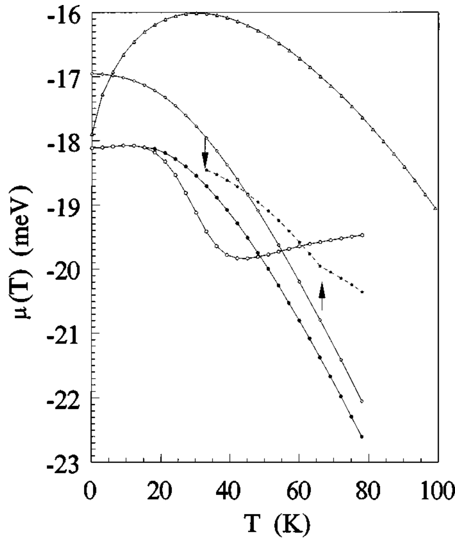

FIG. 2. The chemical potential $\mu(T)$ versus T for the discrete level case (Δ) from Eq. (8) and for several impurity band case using Eq. (9). The discrete level case neglects excited $1s$ bands. It shows that CB states do not push $\mu(T)$ negative until $T>80$ K. For the impurity band case the curves [○, Sommerfeld expansion, ● numerical integration] are based on the DOS in Fig. 1. $\mu(T)$ is pushed negative by the larger DOS well above $\mu(T)$ from the $1s$-T_2, $1s$-E, and UHB states. The slight rise in $\mu(T)$ for $T<15$ K results because $E_F=\mu(0)$ lies below $E_{\min}$ in $N(E)$. A second case (◇) with slightly broader bands and $E_F-E_{\min}=1.05$ meV shows a small negative slope for $T<15$ K and a slightly greater change $\Delta\mu$ at 78 K. When $N(E,T)$ becomes smaller (between the arrows) below E_{CB} at higher T, $\mu(T)$ drops less rapidly (⋆) and could flatten for $40<T<80$ K.

falling almost as T^2. The curve (○) shows the same calculation using the Sommerfeld expansion technique using the derivatives of $N(E)$ up to d^6N/dE^6 obtained directly by numerical differentiation of $N(E)$ in Fig. 1. Another case (◇) for larger band widths and a shallower minimum with $E_F-E_{\min}=1.05$ meV exhibits a small negative slope for $T<20$ K and an overall change $\Delta\mu=-5.1$ meV between 0 and 78 K. For the same band parameters, but including only the LHB and UHB ($E_{\min}=-13.0$ meV) $\mu(T)$ increases from -14.7 meV at 0 K to -13.0 meV at 78 K, but with a substantial decrease in $d\mu(T)/dT$ as $\mu(T)$ approaches $E_{\min}$.

For the impurity band cases in Fig. 2 the contribution from the conduction-band (CB) states above $E_{\text{CB}}=0$ is very small. At $T=75$ K the CB contribution to the numerator $\int N(E)(E-\mu(T))f(1-f)dE$ is 2.4% for $\mu=-22.3$ meV and 4.75% for $\mu=-18.1$ meV. The n_{CB} correction for the denominator is in the same range. At $T=75$ K and $\mu=-18.7$ meV, $n_{\text{CB}}=1.7\times10^{17}/\text{cm}^3$, or only 2% of N_D for the 8.41 sample. The maximum in $N(E)$ at $E\sim-4$ meV of $3.28\times10^{18}/\text{cm}^3$-meV is large compared to $N_{\text{CB}}(E)\propto(E-E_{\text{CB}})^{1/2}$ for E just above E_{CB}. $N_{\text{CB}}(E)$ only becomes comparable to max$[N(E)]$ for $E\sim+200$ meV. The large decrease in $\mu(T)$ for the Si:As impurity band case results directly from the $1s$-T_2 and $1s$-E bands. For the Hubbard band case (single valley) $\mu(T)$ would remain above $\mu(0)$ for T up to 75 K.

A second crucial point about the results in Fig. 2 for the impurity band case is that $N(E)$ was assumed rigid and independent of T. Experimental data show big increases in the low-frequency dielectric response $\epsilon'(N_D,\omega,T)$ at relatively low T resulting from hopping. For $T>25$ K many electrons are excited above E_c and $\epsilon'(N_D,q,\omega,T)$ is not well characterized experimentally. However, for large f_a $\epsilon(T)=\epsilon_h-(\omega_p\tau)^2$ exhibits a plasma contribution where $\omega_p^2=4\pi e^2n_a/m^*$. With a significant increase in $\epsilon'(N_D,q,\omega,T)$ at intermediate T for $q\sim\pi/d$ $[d=N_D^{-1/3}]$ the enhanced screening may push the $1s$-T_2, $1s$-E, and UHB up in energy and these bands may no longer be bound below E_{CB}. Qualitatively $N(E,T)$ for E just below E_{CB} would decrease, thus reducing the negative decrease in $\mu(T)$. A sufficiently large decrease in $N(E,T)$ between $E_{\min}$ and E_{CB} can cause $\mu(T)$ to flatten to a new asymptotic value $\mu(T^*)$ for $T>T^*$. An example is shown in Fig. 2 where the $1s$-T_2 and $1s$-E $N(E)$ are reduced at 33 K and again at 66 K, thus leading to a nearly linear $d\mu/dT\sim-0.5$.

IV. EXPERIMENTAL RESULTS

For the data taken between 4.2 and 77 K the samples were mounted in thermal contact with a Cu block thermal reservoir encased in a vacumn can containing ^{4}He exchange gas. A noninductive heater coil of manganin wire was used to heat the Cu block above 4.2 to 77 K. The sample leads and the thermometer leads were heat sunk to both the external liquid He reservoir and to the Cu block. The calibrated $(1.4<T<100\text{ K})$ Ge resistance thermometer was mounted in a hole in the Cu block. The absolute accuracy of the Ge thermometer was $\pm0.2\%$. The LD δ_t was calculated from the expression $\delta=-(1/\sigma(T_2)T_2)[\sigma(T_3)-\sigma(T_1)]/[1/T_3-1/T_1]$. For $\sigma(T)$ changing slowly with T this expression gives reliable values of $\delta_t(T)$. For the data taken below 4.2 K a specific effort was made to take points equally spaced in $1/T$. For the data for $T>10$ K the data was taken in equal intervals of ΔT. As an example, for $\Delta T=T_3-T_1=1.0$ K at $T\sim20$ K the maximum uncertainty in $\Delta(1/T)$ is of order 7.7% assuming thermal equilibrium and sufficiently low power dissipation to ensure Ohmic conduction.

The δ_t vs $1/T$ data for $1/T<0.1$ taken from Fig. 6 in SKC for four insulating Si:As samples, which has been smoothed and replotted in Fig. 3, shows the high and intermediate temperature regions. The latter region is of particular interest because δ_t is decreasing with increasing $1/T$, whereas at high $T\delta_t\propto1/T$ and at low $T[T<5\text{ K}]\delta_t\propto(1/T)^m$ with $m\sim1/4$. The intermediate region was not satisfactorily explained in SKC, but can be readily explained with Eq. (2). In this region $\delta_a\gg\delta_h$, but σ_a/σ_t is dropping rapidly with $1/T$, thus causing $\delta_t\sim(\sigma_a/\sigma_t)\delta_a$ to decrease with $1/T$ until $(\sigma_a/\sigma_t)\delta_a\sim(\sigma_h/\sigma_t)\delta_h$, below which δ_t reaches a minimum and then rises slowly with $\delta_t\sim\delta_h$. In the intermediate region σ_a/σ_t is falling exponentially with $1/T$ while δ_a/δ_h is only increasing as $(1/T)^{1-m}$. Because the δ_t vs $1/T$ data can be satisfactorily explained with only the two components $\sigma_a(T)$ and $\sigma_h(T)$ this provides the justification for the deconvolution of $\sigma_a(T)$ and $\sigma_h(T)$ and a direct determination of $\delta_a(T)$ and $\delta_{a,c}(T)$.

Two features of the original SKC data should be mentioned. First, the $\Delta\sigma=\sigma_{n=1}-\sigma_n$ shows and even-odd variation of about 10% that accounts for the bimodal feature of the SKC data in Fig. 6 for the 7.57 and 7.90 samples for

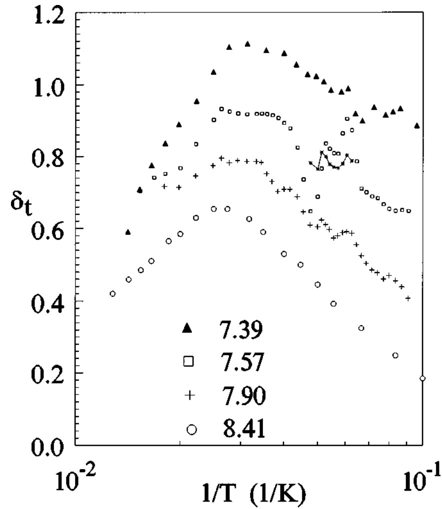

FIG. 3. The smoothed LD δ_t versus $1/T$ for the four samples in the high and intermediate T regions. Larger data scatter occurs for smaller intervals of ΔT. The s-like ''resonance'' on the 7.57 curve is believed to result from an experimental artifact and is partially removed by removing the bump in $\sigma_t(T)$ [more obvious $\sigma_a(T)$] for $0.05<1/T<0.062$ K.

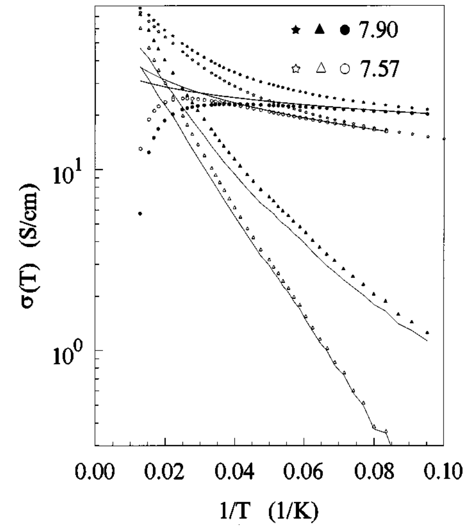

FIG. 4. The conductivity contributions versus $1/T$ for the 7.57 and 7.90 samples. Shown are σ_t (stars), $\sigma_{h,c}$ (●,○), $\sigma_{a,c}$ (▲,△), σ_h (solid lines), and σ_a (solid lines). The Mott VRH parameters A and T_0 for σ_h were determined from the data fit in SKC for $s=0$.

$0.05<1/T<0.10$ that could result from an even-odd variation in the temperature interval $\Delta T=T_{n+1}-T_n$. This is removed by the smoothing of δ_t. Second, the 7.57 sample exhibits an s-like ''resonance'' feature for $0.055<1/T<0.066$ that is believed to be an experimental artifact resulting from a non-Ohmic effect from excessive applied current for eight $\sigma(T)$ points that show a bump for $0.055<1/T<0.070$. Most of this ''resonance'' is removed by removing the bump. The smoothing procedure actually broadens the width of the ''resonance.'' Despite these experimental difficulties, which only become obvious in the LD plots, the overall trends of $\delta_t(T)$ are well established.

Figure 6 in SKC (Ref. 13) shows a minimum in δ_t vs $1/T$ at a temperature $T^*(n)$ with $T^*\sim10$ K for $n=7.39\times10^{18}$/cc and $T^*\sim3$ K for the 8.41×10^{18}/cc sample. The minimum shifts to smaller T as $n\rightarrow n_{c-}$ because of the rapid decrease in T_0 as $n\rightarrow n_{c-}$. An important consideration at higher temperatures is whether the weighting factor σ_h/σ_t becomes small enough at high T ($T>50$ K) so that one obtains $\delta_t\sim\delta_a$ at high T. The data and analysis show this is not the case if the low temperature form of Mott VRH is assumed to hold at higher T well above 10 K. The magnitude of the activation energies obtained suggests an increasingly large fraction f_a of electrons will be excited above the mobility edge at energy E_c with increasing T. E_a will be obtained from the lower temperature data [$1/T>0.05$] where $\mu(T)$ is nearly constant (see Fig. 2) and therefore $E_a(n)$ is E_c-E_F. In the empirical expression for $f_a(n,T)$ B and q, which are coupled, will be determined from the data at low enough T that f_a is small using $\sigma_{a,c}=n_a e\mu_{a,c}(T)=nef_a\mu_{a,c}(T)$. B is directly related to the DOS $N(E_c)$. Based on the possibility of an increasing DOS above E_c, an intermediate value $q=1.25$ was initially assumed and this yielded $B=0.0938\,\mathrm{meV}^{-1}$ for $T_k=1$ K. The strongest n dependence of $f_a(n,T)$ results from the activation energy $E_a(n)$, which is experimentally determined. One also expects some n dependence of $N(E_c)$, but this information is not known and assumptions about $N(E_c,n)$ are speculative. $N(E_F,n)$ can be obtained from low-T specific heat results, but that is not possible for $N(E_c)$. The Si:As data shown below yields δ_a values measurably larger than δ_t, thus leading to significant increases in the activation energy ϵ_a using the LD technique and Eq. (2).

Values of σ_a, $\sigma_{a,c}$, σ_h, and $\sigma_{h,c}$ for the four samples [7.39, 7.57, 7.90, and 8.41×10^{18}/cc] shown in Figs. 2 and 6 in SKC have been calculated using $\sigma_a=\sigma_t-\sigma_h$, $\sigma_{a,c}=\sigma_t-\sigma_{h,c}$, and $\sigma_{h,c}=\sigma_h(1-f_a)$ above and the parameters A and T_0 for the Mott VRH contribution [for $s=0$ case] determined from the data for $0.5<T<5.0$ K in SKC. The results for $\ln\sigma(T)$ versus $1/T$ are shown in Fig. 4 for two samples [7.57 and 7.90]. For the more dilute 7.57 sample σ_a shows a reasonable fit to activated behavior with a single value of E_a, although small deviations from a pure exponential fit are observed. However $\sigma_{a,c}(\Delta)$ shows some upward correction which the LD analysis will attribute to a prefactor dependence. The 7.90 sample (▲) and also the 8.41 sample [data not shown] exhibit significant deviations from a pure exponential fit, which might be caused by more than one activation energy or by the temperature dependence of $E_a(T)$ through $E_c(T)$ and/or $\mu(T)$, but further discussion will follow the presentation of the LD data. $\sigma_t(T)$ data for the 7.57 and 7.90 samples is also shown in Fig. 4. The results suggest there is still a significant contribution from $\sigma_h(T)$ for $T>40$ K. The slopes of $\ln\sigma_t$ and $\ln\sigma_a$ or $\ln\sigma_{a,c}$ vs $1/T$ are quite different, suggesting problems with obtaining activation energies from the slopes of the $\ln\sigma_t$ vs $1/T$ curve. For the 7.90 sample at 77.4 K the analysis shows $\sigma_a\sim0.6\sigma_t$, however, $\sigma_{a,c}\sim0.93\sigma_t$. The behavior of $\sigma_{h,c}(T)$ shows a broad maximum located at $T_{\max}\sim50$, 38, 24, and 12 K for the 7.39, 7.57, 7.90, and 8.41 samples, respectively. This shift in $T_{\max}$ with density is explained by the rapidly decreasing Mott VRH T_0 (see Table I). The crossing of the curves for both σ_h and $\sigma_{h,c}$ for the two samples in Fig. 4 results from the density dependence of the Mott VRH prefactor $A(n)$, which increases with decreasing n. The rapid drop in

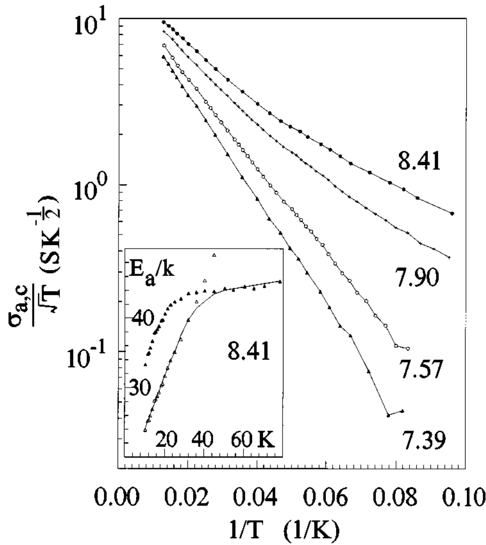

FIG. 5. $\sigma_{a,c}/\sqrt{T}$ versus $1/T$ is shown for the 7.39, 7.57, 7.90, and 8.41 samples. The 7.39 and 7.57 cases yield a single activation energy while the 7.90 and 8.41 cases show an activation energy that changes with T, probably resulting from the T dependence of $E_c(T)$ or $\mu(T)$. The inset shows $E_a(T)$ for the 8.41 sample found from $E_a(T)=T[\ln A(p)-\ln(\sigma_{a,c}/T^p)]$ with $p\sim 0.5$. (△) for $T>40$ K and $p=1.17$ (▲) for $T>30$ K. The solid line is the best overall fit for $E_a(T)$.

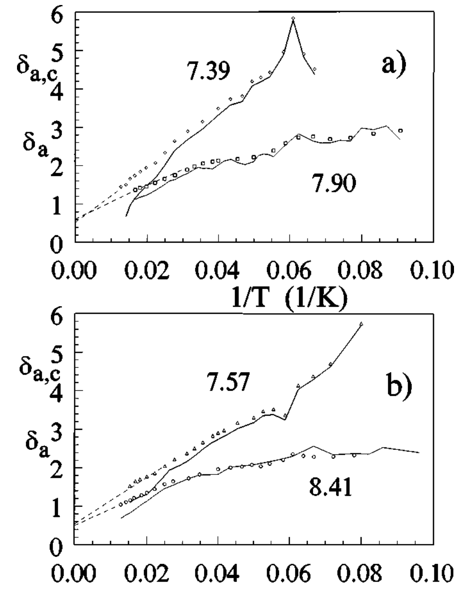

FIG. 6. LD for the activated component $\sigma(T)$ versus $1/T$ for (a) 7.39 and 7.90 samples; (b) 7.57 and 8.41 samples. The solid lines are the uncorrected $\delta_a(f_a=0)$ and show a falloff at small values of $1/T$. The peaks and dips for $1/T>0.05\,\mathrm{K}^{-1}$ result from errors in δ_t, probably due to errors in the temperature intervals ΔT. The $\delta_{a,c}$ for the 7.90 and 8.41 samples show one activation energy at high T and a T dependent $E_a(T)$ for $T<36$ K.

$\sigma_{h,c}$ is determined by the factor $f_a(n,T)$ with the most rapid drop occurring for the smallest activation energy. The rapid drop in $\sigma_{h,c}(T)$ for $T>2T_{\max}$ depends critically on the magnitude of $1-f_a(n,T)$ and is very sensitive to the correct value of $E_a(n)$. Nevertheless, this high-temperature correction to Mott VRH is essential and is far more important than other prefactor T dependences for n just below n_c. It is only the fraction $n_h/n=1-f_a$ of the donor electrons that can be involved in hopping because the fraction f_a above the mobility edge E_c are involved in itinerant electron transport in the impurity band.

It will be shown from the LD plot of $\delta_{a,c}$ versus $1/T$ that the exponent p of the prefactor of $\sigma_{a,c}$ is close to 0.5. This result agrees with the prefactor dependence of $f_a(n,T)[f_a \propto T]$ and $\mu_{a,c}\propto T^{-1/2}$ (see Fig. 7). Thus, a more reliable determination of the activation energy $E_a(n)$ associated with $\sigma_{a,c}$ can be obtained from a plot of $\sigma_{a,c}/T^{1/2}$ versus $1/T$ as shown in Fig. 5 for the four samples. The 7.39 and 7.57 samples are well characterized by a single activation energy. On the other hand, the 7.90 and 8.41 samples exhibit a T-dependent $E_a(n,T)$. The inset in Fig. 5 demonstrates these samples can be fit by a high-T $E_a(T)$ that is slowly varying for $T>50$ K and a low-T $E_a(T)-E_a(0)\propto T$ for $T<25$ K. These activation energies are listed in Table I. The 7.90 and 8.41 samples show $\mu_{a,c}\sim$constant in the low-T range. This suggests plotting $\sigma_{a,c}/T$ versus $1/T$ for the low-T range. It is unlikely that $dE_a/dT\sim$constant continues to $T=0$ K. The results in Fig. 5 also illustrate the difficulties in accurately determining E_a as $n\rightarrow n_{c-}$.

V. DISCUSSION

Using the experimental values of $\sigma_t(T)$, calculated values of σ_h and δ_h extrapolated from the low T region, and smoothed experimental values of δ_t from Fig. 3 one calculates values of $\delta_a(T)$ using Eq. (1a) and $\sigma_a=\sigma_t-\sigma_h$. Correspondingly, $\delta_{a,c}$ is calculated directly from the data for $\sigma_{a,c}$ using $\delta_{a,c}\equiv d\ln\sigma_{a,c}/d\ln T$ rather than using Eq. (7) because of the lack of knowledge of the correction terms. The results for the four samples are shown in Fig. 6. The solid lines show $\delta_a(T)$, while the data points represent $\delta_{a,c}(T)$. The slopes, which determine the activation energy (energies), monotonically decrease with increasing N. Because of the subtractions involved there is more data scatter at larger values of $1/T$ where the quantity $\delta_t-(\sigma_{h,c}/\sigma_t)\delta_{h,c}$ [$\delta_t-(\sigma_h/\sigma_t)\delta_h$ for the case without corrections] is small and σ_a/σ_t is also small. The main problem in the analysis are the larger errors in $\delta_t(T)$ at larger values of $1/T$, which was not fully appreciated during data collection. The wiggle for the 7.57 sample for $0.060<1/T<0.070\,\mathrm{K}^{-1}$ reflects the s-like resonance in Fig. 3. The scatter is less for the 8.41 sample for $1/T<0.06\,\mathrm{K}^{-1}$ because of larger intervals $\Delta(1/T)$. The difference $\delta_{a,c}-\delta_a$ is very small for $1/T>0.05\,\mathrm{K}^{-1}$ because $\delta_{a,c}-\delta_a\propto f_a(n,T)$ and $f_a(n,T)$ becomes small as $T\rightarrow 0$. At the largest T for $1/T<0.02\,\mathrm{K}^{-1}$ there is an appreciable difference between the slopes of $\delta_{a,c}$ and δ_a suggesting different activation energies at high T with and without the $f_a(n,T)$ correction. The principal effect of the correction factor $f_a(n,T)$ is the removal of the droop in the δ_a vs $1/T$ curves at small values of $1/T$ which is largest for the 7.39 and 7.57 curves. All of the curves for $\delta_{a,c}$ show an intercept near $p\sim 1/2$ as $1/T\rightarrow 0$. In addition the slopes for the 7.39 and 7.57 samples are reduced indicating a reduction in the activation energy $E_{a,c}(n)$. The data suggest a more complex situation for the 7.90 and 8.41 samples [at $n/n_c\sim 0.92$ and 0.98, respectively] because for $1/T>0.03\,\mathrm{K}^{-1}$ the slope decreases with increasing $1/T$ consistent with the inset in

TABLE I. Activated and variable-range-hopping parameters.

Sample $10^{18}/\mathrm{cm}^3$	T_0 (K)	R_h/ξ $T_{\max}$	Δ_h (meV) $T_{\max}$	E_a (meV) Ref. 6	E_a (meV) Fig. 5	$f_{a,\mathrm{calc}}$ $T=25$ K	$E_{a,c}$ meV	p[a]
7.39	1470	0.87	2.44	3.9	6.04 ± 0.1	0.018	6.2 ± 0.2	0.50
7.57	278	0.62	1.30	3.8	5.04 ± 0.1	0.029	5.3 ± 0.2	0.57
7.90	14.1	0.38	0.29	3.4	2.6 ± 0.2	0.081	2.9 ± 0.2[b]	0.62
					4.0 ± 0.2		4.1 ± 0.4	
8.41	0.136	0.12	0.08	2.6	2.0 ± 0.2	0.143	2.1 ± 0.2[b]	0.50
					3.5 ± 0.2		3.9 ± 0.4	

[a]Errors in p are ± 0.1, but are coupled to errors in $E_{a,c}$.
[b]At $T=11\,\mathrm{K}-E_a(T)$ linear in T for $10<T<32\,\mathrm{K}$.

Fig. 5. This supports a continuously varying $E_a(n,T)$ resulting from a T-dependent $\mu(T)$. The larger slopes for $1/T<0.03$ are affected by the f_a correction. Using the data for $1/T>0.04\,\mathrm{K}^{-1}$ and ignoring the downward curvature for $1/T<0.04\,\mathrm{K}^{-1}$ one would obtain extrapolated intercepts $p\sim 1.2$ for the 7.90 and 8.41 samples. The uncorrected δ_a results for $1/T<0.025\,\mathrm{K}^{-1}$ yield $p\sim 0$ for 8.41 sample and negative values of p for the 7.39 and 7.57 samples. All of the activation energies are listed in Table I. A more subtle issue concerns the sign of $\delta_{a,c}-\delta_a$ from Eq. (5). $\delta_{a,c}-\delta_a>0$ for the 7.39, 7.57, and 7.90 samples (with the exception of two points for 7.90 where the errors in δ_a are large). The 8.41 case has $\delta_{a,c}-\delta_a>0$ for $T>22\,\mathrm{K}$ and $\delta_{a,c}-\delta_a<0$ for $T<22\,\mathrm{K}$ (except for one point). This is consistent with $\mu_{a,c}(T)$ reaching a maximum (see Fig. 7) near $T\sim 25\,\mathrm{K}$ and the quantity $[\delta_h - d\ln\mu_{a,c}/d\ln T]$ changing sign for $20<T<23\,\mathrm{K}$.

The corrected $E_{a,c}$ values are $50\pm 10\%$ larger than inferred from the slope of $\ln\sigma_t$ vs $1/T$ in SKC for the 7.39 and 7.57 samples. The smaller of the two activation energies is scaling toward zero with $(1-n/n_c)$ faster than values obtained in SKC. The presence of bands associated with the $1s$-T_2 and $1s$-E excited donor states lying between E_c and the conduction-band edge at E_{CB} needs to be considered. It seems unlikely, based on the DOS in Fig. 1, that these bands can account for structure in the DOS above E_c that gives rise to more than a single activation energy. It is plausible, though not possible, to prove in the absence of an accurate DOS $N(E,T)$, that the larger activation energy at larger values of T arises from the drop in $\mu(T)$ at larger values of T. The intercept of $\delta_{a,c}$ as $1/T\to 0$ yields the exponent p of the prefactor of $\sigma_{a,c}(T)$. Figure 6 yields for the four samples $\langle p\rangle\sim 0.55\pm 0.1$. This is consistent with the prefactor of n_a (T^q, $q\sim 1.15$) and $\mu_{a,c}\propto T^{-s}$ ($s\sim 0.55$), as discussed below, in the region $T>50\,\mathrm{K}$. The s value is close to the Conwell-Weisskopf (CW) prediction[24] for ionized impurity scattering for this density and T regime. The CW prediction was originally derived for itinerant electrons in the host conduction band but it should also apply to itinerant electrons in the impurity band, but with different parameters such as the effective mass m^*. The simplest explanation for a T-dependent activation energy, as seen in Figs. 4 and 5 for the 7.90 and 8.41 samples, results from $E_a=E_c-\mu(T)$ with $\mu(T)$ (or E_c) changing by about 1.5 meV for $20<T<78\,\mathrm{K}$. Alternatively, for two contributions to σ_a, namely, $\sigma_a=CT^q e^{-Ea/kT}+DT^\tau e^{-(Ea+W)/kT}$, where W could be the splitting between two separate mobility edges, when one calculates the LD for δ_a one obtains $\delta_a\sim q+E_a/kT$ for $W/kT\gg 1$ and $\delta_a\sim r+(E_a+W)/kT$ for much smaller values of W/kT. The expression for $\delta_a(T)$ involves a crossover function $\phi(T)/[1+\phi(T)][\phi(T)=(D/C)T^{\tau-q}e^{-W/kT}]$. This approach can be shown to be inconsistent with the 7.90 and 8.41 results where for $T<30\,\mathrm{K}$ $E_a(n,T)-E_a(n,0)\sim C(n)T$. As already mentioned one expects only a single mobility edge above E_F $[\mu(T)]$.

Values of the activated electron conductivity mobility $\mu_{a,c}$ are readily obtained from $\mu_{a,c}=\sigma_{a,c}/\mathrm{ne}f_a=(1/\mathrm{ne})[(\sigma_t-\sigma_h)/f_a+\sigma_h]$. Since $\sigma_h(T)$ varies slowly with T the key to the T dependence of $\mu_{a,c}$ rests with the ratio $(\sigma_t-\sigma_h)/f_a$. For the more dilute samples with larger E_a, f_a drops more rapidly than $\sigma_t-\sigma_h$ with decreasing T and $\mu_{a,c}(T)$ increases. For the 7.90 sample $\mu_{a,c}$ shows little no change for $14<T<30\,\mathrm{K}$ implying $\sigma_t-\sigma_h$ and f_a are changing at virtually the same rate with T. The results for $\mu_{a,c}(n,T)$ in Fig. 7 indicate a trend toward a universal behavior at the highest T for $T>50\,\mathrm{K}$ that shows $\mu_{a,c}\propto T^{-s}$ with $s=0.55$, 0.48, 0.54, and 0.57, respectively, for the 8.41, 7.90, 7.57, and 7.39 samples. These exponents are close to the Conwell-Weisskopf prediction $[s=1/2]$ for ionized impurity scattering for high densities at relatively low T where lattice phonon scattering is negligible. The magnitude of $\mu_{a,c}$ at 77 K is close to the Conwell-Weisskopf value for Si at 77 K [see Figs. 9–11 in Shockley[25]]. The 7.57 and 7.39 samples show a slightly more rapid rise at low T than $T^{-1/2}$. This upward deviation is in agreement with Conwell-Weisskopf theory. Their expression, originally derived for electrons in the host CB is

$$\mu_I=C[\epsilon^2(kT)^{3/2}/N_I]/f(X_{\mathrm{CW}}), \tag{10}$$

where the constant $C=(8/\pi)(2/\pi)^{1/2}/e^3 m^{*1/2}$, $f(X_{\mathrm{CW}})=\ln(1+X_{\mathrm{CW}})$, ϵ is the host dielectric constant minus a plasma contribution that is important when f_a is large, and N_I is the density of ionized impurities, and $X_{\mathrm{CW}}=(3\epsilon kT/e^2 N_I^{1/3})^2$. For the impurity band case $N_I=f_a n+2N_A$, but the compensation $K=N_A/N_D$ is believed to be very small $[K<10^{-4}]$ so that $N_I\sim f_a n$ except at the very lowest temperatures. The CW theory does not take account of screening resulting from the space charge distribution around an ionized donor impurity. A refined treatment including this screening has been given by Brooks-Herring[26] (BH). In the BH treatment the denominator in Eq. (9) is replaced by $[\ln(1+X_{\mathrm{BH}})-X_{\mathrm{BH}}/(1+X_{\mathrm{BH}})]$, where $X_{\mathrm{BH}}=24m^*(kT)^2/ne^2\hbar^2$. The BH result for low T and large

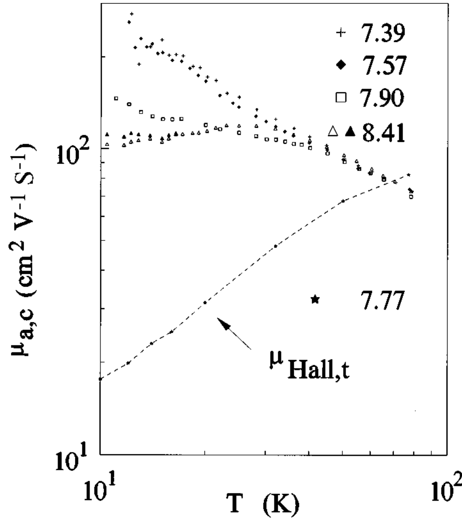

FIG. 7. The mobility $\mu_{a,c}=\sigma_{a,c}/enf_a$ for samples 8.41, 7.90, 7.57, and 7.39 versus T in the intermediate regime $[d\delta_t/d(1/T)<0]$ and the high-T regime $[d\delta_t/d(1/T)\sim E_a/k>0]$. $f_a(n,T)$ was determined from Eq. (3) using the empirical form and activation energies from Fig. 3. Also shown is the measured Hall mobility for a 7.77 Si:As sample (Ref. 30). The slope of $\mu_{a,c}$ vs T for $40\,\mathrm{K}<T<70\,\mathrm{K}$ is in approximate agreement with the CW prediction (Ref. 24).

$n(X_{\mathrm{BH}}\ll 1)$ yields $\mu_I\propto T^{-5/2}(n^2/N_I)$, which is a very different result than the CW result in the low-T, high doping regime. It has been well known[27] the BH theory deviates strongly from the experimental results in this regime. Chattopadhyay and Queisser[28] have given a detailed review of the features and corrections affecting ionized impurity scattering. The best agreement with the Si:P results[29] at $T=77\,\mathrm{K}$ in this doping regime has been obtained by Sanborn, Allen, and Mahan[30] using a random-phase approximation and calculation of the phase shifts. However, these authors assumed all the electrons in the CB at $T\sim 77\,\mathrm{K}$. For the Si:As results here itinerant electrons are predominantly in the impurity band.

For $X_{\mathrm{CW}}\ll 1$ Eq. (10) yields $\mu_I\propto T^{-1/2}/N_I^{1/3}$. However, $N_I^{1/3}\sim[nf_a(n,T)]^{1/3}$ is a function of T and the parameter $X_{\mathrm{CW}}>0.55$ for the 7.57 sample and $X_{\mathrm{CW}}>0.3$ for the 7.9 sample for $10<T<78\,\mathrm{K}$ implying the expansion $\ln(1+X_{\mathrm{CW}})\sim X_{\mathrm{CW}}$ is not a good approximation. Moreover, $E_a/kT<0.6$ at 78 K for the 7.90 sample meaning one is not in the classical regime. The general Mansfield[31] expression for the conductivity σ_I resulting from ionized impurity scattering for arbitrary degeneracy can be adapted for scattering in the impurity band and is discussed in Appendix C. An important special case relevant to the high-T regime occurs when $X\ll 1$ and $f(X)=\ln(1+X)\sim X=(\epsilon\eta kT/e^2N_I^{1/3})^2$. This allows an evaluation of the integral in (C2) yielding

$$\sigma_I=(e^2/h)[4N(E_c)/3N_I^{1/3}](\hbar^2kT/2m^*)^{1/2}F_{-1/2}(\eta^*), \tag{11}$$

where the Fermi integral $F_{-1/2}(\eta^*)=\int_0^\infty \eta^{-1/2}(e^{\eta-\eta^*}+1)^{-1}d\eta=\sqrt{\pi}e^{\eta^*}[1-e^{\eta^*}/\sqrt{2}+e^{2\eta^*}/\sqrt{3}-\cdots]$ $(\eta^*=-E_a/kT)$. The result in Eq. (11) is almost identical to the empirical expression $\sigma_{a,c}=nef_a\mu_{a,c}$ since $f_a=N(Ec)kTF_0(\eta^*)$ $[F_0=\ln(1+e^{\eta^*})]$ and $d\ln\mu_{a,c}/d\ln kT\sim -0.5$ at higher T. The difference in the T dependence is small for $T>30\,\mathrm{K}$. The experimental results (from Figs. 4 and 5) for $\sigma_{a,c}$ for $T>40\,\mathrm{K}$ can be compared directly with Eq. (11) and directly yield estimates of product $N(E_c)(m/m^*)^{1/2}$. These estimates are shown in Table II. The decoupling of $N(E_c)$ and m^*/m requires an additional assumption. The original parameters used in $f_{a,\mathrm{emp}}$ were based on $N(E_c)/n=\mathrm{constant}=0.094\,\mathrm{meV}^{-1}$ and $q=1.25=\mathrm{constant}$. The overall analysis suggests q is closer to 1 because $\alpha(T)$ decreases toward zero, either because $E_c(T)$ slides down the $N(E)$ curve toward $E_{\min}$ as T increases, or because $N(E_c(T),T)$ decreases with T, or some combination of both these effects. The results for E_a and for $\mu(T)$ in Fig. 2 suggest a reduction in $N(E)$ for $E>E_c$ at higher temperatures. However, $\alpha(T)$ is not reliably determined since it is a higher order correction. The analysis suggests the original choice $q=1.25$ was too large. The $f_{a,\mathrm{emp}}$, however, seem to give reasonable results and a 30% reduction in $f_{a,\mathrm{emp}}$ values yields poorer results. A decrease in q to the range 1.00 to 1.05 requires a 50% increase in $N(E_c)$ to maintain the same value of f_a at higher T. The third and fourth columns, which are based on $N_I=nf_a$, in Table II show $N(E_c)$ and m^*/m for the case $N(E_c)/n=0.14\,\mathrm{meV}^{-1}$, which is 50% larger than the original choice. The results show $N(E_c)$ increasing with n and m^*/m decreasing slightly with n. The m^*/m values are larger than $m^*/m=0.26$ for the CB valleys and they have the right n dependence. For this strongly overlapping impurity band case one should not assume $N(E_c)\propto m^*$. Such an assumption would lead to a much stronger change in $N(E_c)$ with n and would require m^*/m to increase with n (a factor of 2 between 7.39 and 8.41). This is inconsistent with the notions the bands must narrow as n is decreased. The fifth and sixth columns are based on $N_I=n$. These results are similar to those in 3 and 4, but with almost no variation in m^*/m with n. When one attempts to explain the T dependence of σ_I in Eq. (11) there is a substantial

TABLE II. Estimate of $N(E_c)$ and (m^*/m) parameters for $T=78\,\mathrm{K}$.

n	$N(E_c)(m/m^*)^{1/2}$	$N(E_c)/10^{18}$	m^*/m	$N(E_c)(m/m^*)^{1/2}$	m^*/m
8.41	1.92×10^{18} [a]	1.20 [a,b]	0.39	0.39 [a,c]	0.35
7.90	1.69×10^{18} [a]	1.13 [a,b]	0.44	1.81 [a,c]	0.38
7.57	1.63×10^{18} [a]	1.08 [a,b]	0.44	1.83 [a,c]	0.34
7.39	1.56×10^{18} [a]	1.05 [a,b]	0.45	1.82 [a,c]	0.34

[a]Units $\mathrm{meV}^{-1}\text{-}\mathrm{cm}^{-3}$.
[b]Based on $N_I=nf_a$.
[c]Based on $N_I=n$.

difference in the result depending on whether one chooses $N_I=nf_a(n,T)$ or $N_I=n$. The first choice $N_I=nf_a$ would require an nearly linear decrease in $N(E_c(T),T)$ with decreasing T for $25<T<78\,\mathrm{K}$ for $\sigma_{a,c}=\sigma_I$. This cannot be ruled out, but seems like too large a change in $N(E_c)$ with T. Assuming $N_I=n$ would require only a 6% reduction between 78 and 36 K and an additional 16% reduction between 36 and 25 K. However, the choice $N_I=n$ is not valid over the entire sample and would have to be justified with substantial inhomogeneity that becomes more important with decreasing T. This is consistent with percolation ideas and with Poisson statistics for random systems where the conducting channels would have N_I close to n and the insulating regions would have $N_I \ll n$. The uncertainty in the decoupling of $N(E_c)$ and m^*/m is likely less than 30% [a 20% increase in $N(E_c)$ would require a 44% increase in m^*/m]. Mansfield's expression, adapted for the impurity band case and using phase shifts, yields $\sigma_{I,ps}$ [Eq. (C5)], which can also be compared with the data at $T=78\,\mathrm{K}$. The first case $(N_I=nf_a)$ gives a result independent of $N(E_c)$ and yields m^*/m values 0.36 and 0.19 for the 8.41 and 7.39 cases, respectively. The second case $(N_I=n)$ yields $N(E_c)(m^*/m)^{1/2}$ values of 1.71 and and 1.45 for the 8.41 and 7.39 samples. Using the same decoupling scheme as above with $N(E_c)/n=0.14\,\mathrm{meV}^{-1}$ one obtains m^*/m values of 2.03 and 1.88 for the 8.41 and 7.39 cases. The agreement is less satisfactory than above and in both cases m^*/m decreases with decreasing n, an unlikely dependence. More serious problems occur when one tries to explain the T dependence with $\sigma_{I,ps}$. In both cases the T dependence of $\sigma_{I,ps}$ is such that the agreement gets worse as T is decreased. For the first case $\sigma_{I,ps} \propto \sqrt{T}(y/\ln(1+y))x\int$, while for the second case $\sigma_{i,ps} \propto (kT)^{3/2}yx\int$. The integral varies slowly with T. Hence case one has too slow a T dependence while case two has too rapid a T dependence.

This difference between σ_I and $\sigma_{I,ps}$ arises from the energy dependence of the scattering cross section $\langle\sigma\rangle$ where $1/\tau=N_I v\langle\sigma\rangle$. For the CW case $\langle\sigma\rangle_{\mathrm{CW}}=(2\pi/4)N_I^{-2/3}(\ln(1+X)/X)$. This gives a constant geometrical cross section at low energy and falls off with energy $(X\propto E^2)$ for $X>1$. However, $\langle\sigma\rangle_{ps}=(4\pi/k^2)\Sigma_l(l+1)\sin^2(\delta_l-\delta_{l+1})$ is proportional to E for $\delta_0 \propto E$ for small E and falls off roughly as $1/E$ for large E. The different low-energy dependence of $\langle\sigma\rangle$ accounts for the difference in the two results. If $\delta_l \propto k^{l+1}$ then $\langle\sigma\rangle_{ps}$ would approach a constant as $E\to 0$ and the two results would coincide, however, the theoretical basis for this is unclear. The two characteristic lengths in the problem are $d=n^{-1/3}$ and the screening length L_s. When $d<L_s=1/\beta_s$ then the CW cutoff appears to be the dominant effect.

The use of the CW expression, rather than BH, for the function $f(X)$ in the denominator of Eq. (9) also requires additional discussion. The inverse screening length $[V(r)=(e/\epsilon r)e^{-\beta s r}]$ found for the general Mansfield case is $\beta_s=\{(e^2/\epsilon kT)[n_a F_0'(\eta^*)/F_0(\eta^*)]\}^{1/2}$ employing a constant $N(E)$ above E_c. $F_0(\eta^*)=\ln(1+e^{\eta^*})$ is the Fermi integral contained in n_a. Keeping only the first term for n_a in the expansion of $N(E)$ about E_c one obtains $\beta_s=\{e^2N(E_c)/\epsilon[y/(1+y)]\}^{1/2}$. As $T\to 0$ $\beta_s\to 0$ and the screening length L_s diverges since $\eta^*<0$ and $y\to 0$. A numerical comparison of the CW cutoff radius $a_I/2=1/2N_I^{1/3}=1/3n^{1/3}f_a^{1/3}$ reveals $a_I/2$ is always less than L_s for $10<T<78\,\mathrm{K}$. For the 7.90 sample $a_I/2L_s\sim 0.4$ at 72 K and 0.9 at 12 K, while for the 7.57 sample $a_I/2\sim 0.4$ at 72 K and 0.6 at 12 K. If at low T where $f_a \ll 1$ and $\sigma_{a,c}$ is very small the itinerant electron conduction is not homogeneous, but occurs in conducting channels because of the random potential, $a_I/2$ will be reduced causing the ratio $a_I/2L_s$ to be even smaller at low T. In effect, much of the screening is removed by the CW cutoff suggesting the correct $f(X)$ is closer to the CW $\ln(1+X_{\mathrm{CW}})$ than to the BH $\ln(1+X_{\mathrm{BH}})-[X_{\mathrm{BH}}/(1+X_{\mathrm{BH}})]$. The correction to the CW $f(X)$ will slightly reduce $f(X)$ and increase μ_I. However, the analysis still has neglected the strong short-range central cell potential that leads to donor-dependent binding energies. This correction will lead to donor-dependent mobilities such that for the same n $\mu_{a,c}(\mathrm{Si{:}As})<\mu_{a,c}(\mathrm{Si{:}P})$.

If one multiplies $\sigma_t=\sigma_{h,c}+\sigma_{a,c}$ by the total Hall coefficient $R_{H,t}$ and identifies the hopping and activated Hall coefficients as $R_{H,h}$ and $R_{H,a}$ one obtains the relation

$$\mu_{H,t}=(R_{H,t}/R_{H,h})\mu_h+(R_{H,t}/R_{H,a})A\mu_{a,c}, \qquad (12)$$

where $\mu_{H,t}\equiv R_{H,t}\sigma_t$, $R_{H,h}=(A/en_h)\exp(T_{oH}/T)^{1/4}$, based on the theoretical[32] and experimental[33] results [$\mu_h \propto \exp[(T_{oH}/T)^{1/4}-(T_0/T)^{1/4}]$, $R_a=A(n,T)/en_a$ and $R_{H,t}=A(n,T)/en$. $A(n,T)$ is the Hall correction factor that is slightly larger than unity and depends on the type of scattering and degeneracy. $A(n,T)$ doesn't depend on the host CB valley anisotropy because the $1s$-A_1 band is a symmetric sum of the six Si conduction band valleys. The Hall coefficients $R_{H,a}$, $R_{H,h}$, and $R_{H,t}$ are motivated by $n_a+n_h=n$, implying (for $T_{oH}\ll T$) $R_{H,t}^{-1}\sim R_{H,h}^{-1}+R_{H,a}^{-1}$. This relation becomes an equality as $T_{oH}\to 0$ and is better satisfied as $n \to n_{c-}$. Equation (12) can then be rewritten as

$$\mu_{H,t}=(1-f_a)\exp-(T_{oH}/T)^{1/4}\mu_{h,c}+f_aA(n,T)\mu_{a,c}. \qquad (13)$$

In the low-T region ($T<10\,\mathrm{K}$) f_a is negligible and $\mu_{H,t}\sim\exp[-(T_{oH}/T)^{1/4}\mu_{h,c}$. In the intermediate-$T$ region ($10<T<50\,\mathrm{K}$) f_a increases rapidly and accounts for the rapid rise in $\mu_{H,t}$ resulting from the second term in Eq. (13) while the first term is decreasing. In the higher-T region ($T>50\,\mathrm{K}$) the second term in Eq. (13) dominates and $\mu_{H,t}\sim f_aA\mu_{a,c}$. In this regime the hopping term in Eq. (13) is negligible. The above approach following Eq. (12) differs from an approach using $1/\mu_t=1/\mu_{h,c}+1/\mu_{a,c}$ based on the assumption the processes contributing to $\mu_{h,c}$ and $\mu_{a,c}$ are independent. However, because $n_h(T)+n_a(T)=n=N_D-N_A=\mathrm{constant}$ these processes are not independent. The data[34] in Fig. 7 show $\mu_{H,t}\sim 1.13\mu_{a,c}$ for a $7.77\times 10^{18}/\mathrm{cm}^3$ sample, which is consistent with Eq. (13). Using the weighted average of the 7.57 and 7.90 samples at $T\sim 77.6\,\mathrm{K}$ yields $f_a\sim 0.76$ and $A=1.48$, which suggests the value of f_a is about right at $T\sim 77\,\mathrm{K}$. Blatt[35] calculated the Hall factor $A(n,T)=\mu_H/\mu_d$ for n-type Si and finds A increasing from 1.17 at 20 K to 1.55 at 50 K for $n=10^{16}/\mathrm{cm}^3$. For $n=2\times 10^{16}/\mathrm{cm}^3$ he obtains $A=1.12$ at 20 K and and 1.42 at 50 K. At much higher n just below n_c ($n_c=8.57\pm 0.08\times 10^{18}/\mathrm{cm}^3$) the increase in $A(n,T)$ in this temperature range should be smaller. Newman, Hirsch, and Holcomb[36] have obtained values of $A(n,T)$ between 1.4 and 1.5 at 295 K near n_c for Si:As, while del Alamo and

Swanson[37] obtained $A \sim 1.3$ near n_c for Si:P $[n_c = 3.7 \times 10^{18}/\text{cm}^3]$ at RT. With only a small change in $A(n,T)$ between 20 and 77 K, most of the increase in $\mu_{H,t}$ with T results from the increase in $f_a(n,T)$ with T. Based on the empirical formula, $f_{a,\text{emp}}$ will approach unity for T near 90 K depending on the value of E_a $[n=7.57,\ E_a = 5.04\,\text{meV},\ f_a(94\,\text{K}) = 1;\ n=7.90,\ E_a = 4.03\,\text{meV},\ f_a(88.5\,\text{K}) = 1]$. For $T > T_c$ for $f_a(T_c) = 1$ there is no change in f_a (although the relative fractions between the impurity band and the conduction band will continue to change) and $\mu_{H,t}$ will flatten out and change more slowly with T. For $T > T_c$ $\mu_{H,t}/\mu_{a,c}$ $[\mu_{a,c} = \mu_{\text{drift}}]$ will determine $A(n,T)$. The empirical expression $f_{a,\text{emp}}(T)$ might yield an overestimate at 77 K. The higher order terms in the expansion for $f_a = n_a/n$, namely, $\Sigma_{m=2}(1/m!)(d^mN/d^mE)_{Ec}\int(E-E_c)^m f(E,T)dE$ probably do not make a significant correction to $f_a(n,T)$ because $(d^mN/d^mE)_{Ec}$ is positive for $m=2$, but is negative for $m=3$ and 4. However, the expansion approach will break down [just as it did for $\mu(T)$ shown in Fig. 2] for $kT > 1/3(E_{\text{CB}} - E_c) \sim 5\,\text{meV} \sim 60\,\text{K}$. The coefficient $B = 0.00809$ in f_a yields a DOS $N(E_c) \sim 0.77 \times 10^{18}/\text{meV-cm}^3$ that is within $\pm 25\%$ of that shown in Fig. 1 for $3.2 < E_a < 6.0\,\text{meV}$, which provides additional evidence that the empirical values $f_{a,\text{emp}}(n,T)$ are approximately correct.

The nearly flat region $\mu_{a,c}(n,T)$ in Fig. 7 for the 7.90 and 8.41 cases is explained by $\sigma_t - \sigma_h$ and f_a having almost the same T dependence since σ_h is slowly varying and decreasing as T is reduced. For the 7.39 and 7.57 cases, f_a drops more rapidly than $\sigma_t - \sigma_h$ as T is reduced because of the larger nearly constant E_a values, thus causing $\mu_{a,c}$ to continue to rise. Conversely, for the 7.90 and 8.41 cases f_a drops more slowly, particularly because $E_a(T)$ drops linearly with T for $T < 30\,\text{K}$ and E_a/kT increases much more slowly with decreasing T. Eventually, for the $T < 14\,\text{K}$ the 7.90 sample starts to rise more rapidly. The $\mu_{a,c}$ results for $T < 36\,\text{K}$ for 7.90 and 8.41 are rather sensitive to $E_a(n,T)$ and are less reliable than those for $T > 36\,\text{K}$. However, the qualitative trends are correct. Strictly speaking one cannot employ the classical result $\mu_{a,c} = \sigma_{a,c}/enf_a$ when the collision rate is energy dependent. However when the cross section $\langle\sigma\rangle$ is nearly constant over the region where $f(1-f)$ is large this is a reasonable first approximation since then $1/\tau \propto \sqrt{E}$ varies slowly with E. However, $\sigma_{a,c}$ depends much less on f_a and it is better to compare it with theory. One possibly relevant process for a T-independent mobility is the neutral impurity scattering result $\mu_n = e/20\hbar a^*(N_D - N_A)$ of Erginsoy.[38] It yields $\mu_n = 48\,\text{cm}^2/\text{V s}$ for the 7.90 sample and slightly larger values for the 7.57 and 7.39 samples. If neutral and ionized impurity scattering are independent processes (not necessarily true) this implies $\mu_{a,c}^{-1} = \mu_I^{-1} + \mu_n^{-1}$, which would yield $\mu_{a,c} < \mu_n$ since $\mu_n < \mu_I$, but this is not consistent with the data. Either the Erginsoy relation overestimates the scattering from neutral impurities or the itinerant electrons in the percolation channels are spatially separated from most of the neutral impurities. The low T upturn for 7.90 is significant because it rules out a T independent mechanism like neutral impurity scattering.

$f_{a,\text{emp}}(n,T)$ has been calculated with a realistic model, but any T variation of the DOS $N(E,T)$ for E just above E_c has been neglected. Experimentally $f_a = \sigma_{a,c}/ne\mu_{a,c}$ cannot be determined since $\sigma_{a,c}$ depends on f_a and $\mu_{a,c}$ has not been independently determined. However, the LD approach provides a means to obtain $f_{a,\text{exp}}$ using Eq. (5), $\delta_{a,c} \equiv d\ln\sigma_{a,c}/d\ln T$, δ_a [from Eq. (2), not Eq. (1a)], δ_h, σ_h, $\sigma_t - \sigma_h$, and $d\ln\mu_{a,c}/d\ln T$. Although $\delta_{a,c}$ could be calculated from the various terms in Eq. (7) there is only experimental information on the first three, and while $p \sim 0.5$ at high T it is not known throughout the entire range, particularly for the 7.90 and 8.41 samples with a T-dependent E_a. A better procedure is to calculate it from $\delta_{a,c} \equiv d\ln\sigma_{a,c}/d\ln T$ directly from the results for $\sigma_{a,c}$ based on the assumed $f_{a,\text{emp}}$. It is a nontrivial task to separate out the smaller correction terms in Eq. (7) because the fourth and fifth terms have opposite sign and the three parts of the fourth term also can have different signs since one expects $d\mu/dT$ to be negative for $T > 20\,\text{K}$. E_a is known from the results for $\sigma_{a,c}/T^{1/2}$ [or $\sigma_{a,c}/T$ for $p \sim 0$] vs $1/T$. The high-T results ($T > 30\,\text{K}$) suggest $p \sim 1/2$ and this result extends to lower T for the 7.39 and 7.57 samples. Below $T \sim 40\,\text{K}$ the 7.90 and 8.41 sample results suggest $\mu_{a,c} \rightarrow$ constant leading to $p \sim 0$. $dE_a/dT \sim 0$ for the 7.39 and 7.57 cases, but is nonzero and positive in the middle of the T range for the 7.90 and 8.41 samples. The results for the chemical potential $\mu(T)$ in Fig. 2 imply $dN(E_c,T)/dT$ is nonzero (probably negative) for $20 < T < 30\,\text{K}$, but it is not possible to infer how $N(E,T)$ varies quantitatively with T for E just above E_c.

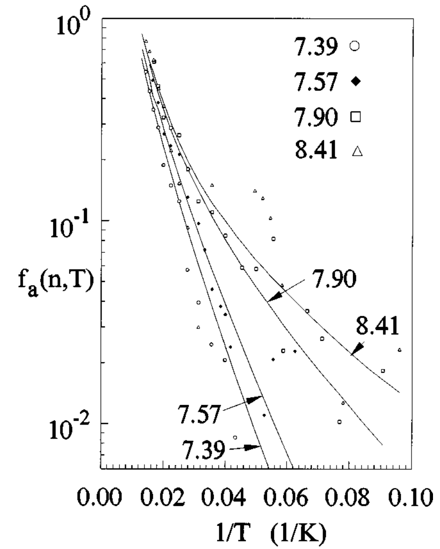

FIG. 8. The fraction $f_a(n,T) = n_a/n$ versus $1/T$ for the 8.41, 7.90, 7.57, and 7.39 samples. The solid lines are based on $f_{a,\text{emp}} = 0.00809T^q \ln(1 + e^{-Ea(n)/T})$ where $q = 1.25$. The $f_{a,\text{exp}}$ values were calculated with Eq. (5) and experimental values of $\delta_{a,c}$, δ_a, $\sigma_t - \sigma_h$, σ_h, and $d\ln\mu_{a,c}/d\ln T$.

The results for $f_{a,\text{exp}}(n,T)$ versus $1/T$ in Fig. 8 exhibit reasonable agreement with the empirical expression (solid line) for $1/T < 0.025$. The scatter increases at lower T [where both $\sigma_t - \sigma_h$ and $\sigma_t\delta_t - \sigma_h\delta_h$ are getting smaller and errors in the latter are increasing, particularly in δ_t], but there are some systematic trends. For the 7.39 and 7.57 samples the $f_{a,\text{emp}}$ values lie below $f_{a,\text{emp}}$ for $T < 30\,\text{K}$. This can be explained by a reduction in $q(T) = 1 + \eta(T)$ as T is reduced, or by a reduction in $N(E_c(T),T)$ (less likely). For $1/T$

$>0.055\,\mathrm{K}^{-1}$ the agreement deteriorates for the 7.57 case. The 7.90 samples shows good agreement down to 20 K. Below 30 K the scatter increases and the $f_{a,\mathrm{exp}}$ points lie both above and below $f_{a,\mathrm{emp}}$, but with more points above $f_{a,\mathrm{emp}}$ than below, the opposite of the low-T trend for the 7.39 and 7.57 cases. The 8.41 case is both the most interesting and difficult case because of the small values of $\delta_h(T)$ and the reversal of sign of $d\ln\mu_{a,c}/d\ln T$ at $28\,\mathrm{K}(1/T=0.036\,\mathrm{K}^{-1})$ shown in Fig. 7. Despite reasonable agreement for $T>50\,\mathrm{K}$, $f_{a,\mathrm{exp}}$ drops precipitously for $0.025<1/T<0.032\,\mathrm{K}^{-1}$. $(\sigma_t-\sigma_h)(\delta_{a,c}-\delta_a)$ in the numerator changes sign at $T\sim 22\,\mathrm{K}$ (see Fig. 4). The small values of both numerator and denominator and the subtractions account for the large deviations in $f_{a,\mathrm{exp}}-f_{a,\mathrm{emp}}$ for $0.033<1/T<0.055\,\mathrm{K}^{-1}$. There is a slight improvement, but with large scatter for $1/T>0.06\,\mathrm{K}^{-1}$. Overall, taking account of the increasing scatter for $1/T>0.04\,\mathrm{K}^{-1}$ and the delicate nature of the subtraction in $\delta_{a,c}-\delta_a$ at lower T the agreement between $f_{a,\mathrm{exp}}$ and $f_{a,\mathrm{emp}}$ is satisfactory.

It is worth speculating about the form of $f_a(n,T)$ as $n\to n_c$ in the low-T regime ($T<10\,\mathrm{K}$). For $N(E-E_c)\sim$ constant $f_a(n_c,T)=N(E_c)kT\ln 2$, while for $N(E-E_c)\propto(E-E_c)^{1/2}$ $f_a(n_c,T)\propto T^{3/2}$. There is a large body of data on many different MIT systems that shows $\sigma(n\sim n_c,T)\propto T^{1/2}$. If one relates these results to $\sigma_{a,c}(n_c,T)$ one would conclude $\mu_{a,c}\propto T^{-1/2}$ for $N(E-E_c)\sim$constant and $\mu_{a,c}\propto T^{-1}$ for $N(E-E_c)\propto(E-E_c)^{1/2}$. This apparently paradoxical notion of diverging mobilities as $T\to 0$ would suggest $1/\tau(n_c)\propto\sqrt{T}$ for $N(E-E_c)\sim$constant and $1/\tau(n_c)\propto T$ for $N(E-E_c)\propto(E-E_c)^{1/2}$. The former is smaller than expected theoretical dependences, while the latter agrees with the $1/\tau$ from electron-electron interaction theory. An alternative approach employs the expression $\sigma(n_c,T)\propto 2e^2/hL(T)$ where $L(T)=[D(n_c,T)\tau(T)]^{1/2}$ [note that $D(n_c,T=0)=0$]. For $D(n_c,T)\propto T$, appropriate for the nondegenerate region ($kT\gg\epsilon_F$), this leads to a result $1/\tau\propto T^2$ analagous to quasiparticle interactions and Fermi-liquid behavior. Using the Einstein relation for a nondegenerate system $D(n_c,T)=kT\mu$ one finds a finite mobility at n_c. This suggests caution in using the relation $\sigma_{a,c}=\mathrm{en}f_a\mu_{a,c}$ in the critical regime as $T\to 0$. Nevertheless, the behavior of $f_a(n_c,T)$ described above is correct as $T\to 0$ and depends only on the form of $N(E-E_c)$.

There has been some disagreement about Mott VRH in the limit $T>T_0$ and $R_h/\xi(n)<1$, where $R_h(T)$ is the hopping length and $\xi(n)$ is the localization length. It has been suggested[39] that in this limit $\sigma(T)$, which is slowly varying with T, but is still a good fit to the Mott law, is not really Mott VRH. The original Mott derivation was for the regime $T_0>T$ and $R_h>\xi(n)$ and included a prefactor T dependence of $\sigma_0(T)\propto(1/T)^s$. Mott's derivation led to a prefactor $\sigma_0(T,n)\propto\Delta R^2$, which after minimization of the exponent yields $\sigma_0\propto\Delta_h R_h^2\propto(kT)^{1/4}(1-n/n_c)^{\nu/4}$. This gives $s=-1/4$ for isotropic envelope functions and $\sigma_0(T,n\to n_c)\to 0$. Neither of these predictions are consistent with the data in the critical regime. The SKC Si:As data shows $|s|<0.04$, while the Si:P low-T data[40] yield $|s|<0.02$. Recently Delahaye, Brison, and Berger[41] have found that i-AlPdRe (icosahedral phase) quasicrystals exhibit Mott VRH in the temperature range 20–600 mK and yield Mott T_0's in the vicinity of 1 mK, or much less than the measuring range. Delahaye *et al.*[41] obtain values of $s<0.01$ and their results more closely approach the case of ''pure'' Mott VRH with $s=0$ than any other experimental results. No known experimental results show $\sigma_0(T,n)\to 0$ as $n\to n_c$. Instead the results show $\sigma_0(n)$ approaching a constant at n_c, and as n is reduced increasing slowly for $0.95<n<n_c$ and more rapidly for $n<0.95n_c$.

An effort[42] was made to extend the MA theory to the critical regime, but still within the pair approximation. In the low-T regime ($T<1$ K) for $1-n/n_c<0.1$ one finds $qR_{ab}\ll 1$ [q the phonon wave number for phonon absorption and R_{ab} the hopping distance between sites a and b] and terms dropped by MA in the dilute limit are no longer negligible. This effort, which neglected the spatial dependence of dielectric screening $[\epsilon(n,r);\epsilon\to\epsilon_h$ as $r\to 0,\epsilon\to\epsilon(n)$ which diverges as $n\to n_{c-}]$ did not yield a sensible dependence for the Mott prefactor as $n\to n_c$. Two new approaches, one based on Mott's phenomenological approach and the second on a different, modified MA approach, lead to a new prefactor dependence $\sigma_0(n,T)\propto f(\Delta,R)$. In this case Mott's ansatz $\Delta\propto R^{-3}$ and minimization leads to a prefactor $\sigma_0(n)$ independent of T and $\xi(n)$ that can describe the density dependence of $\sigma_0(n)$ shown for the Si:As and Si:P data. A detailed theory of VRH in the critical regime and comparison with the most extensive data will be presented elsewhere. All of the data discussed above are in the critical regime where the crossover parameter $x=\Delta_h/2kT=(1/8)(T_0/T)^{1/4}$ is less than 0.44. The pair approximation is likely to be inadequate in the critical regime for n just below n_c. Here $\xi(n)\gg d=N_D^{-1/3}$ and there are of order $(\xi/d)^3$ donor sites within a localization length. A localized eigenstate $\psi_a(\mathbf{r}-\mathbf{R}_a,E_a)=\Sigma_i^m c_{a,i}\phi_i(\mathbf{r}-\mathbf{R}_i)$ with energy E_a, where the $\phi_i(\mathbf{r}-\mathbf{R}_i)$ is a donor wave function localized about the ith donor. A second localized eigenstate $\psi_b(\mathbf{r}-\mathbf{R}_b,E_b)=\Sigma_j^m c_{b,j}\phi_j(\mathbf{r}-\mathbf{R}_j)$ with energy E_b is in the vicinity with $R_{ab}<\xi$. For the 7.39 sample $m\sim 10$ while for the 8.41 sample $m>1000$. The orthogonality requirement $\langle\psi_b|\psi_a\rangle=0$ and $R_{ab}<\xi$ requires the coefficients $c_{a,i}$ and $c_{b,j}$ to be both positive and negative. Calculation of the hopping matrix element $\langle\psi_b|e^{i\mathbf{q}\cdot\mathbf{r}}|\psi_a\rangle$ is complex and features much cancellation (unlike the pair case) because of the fluctuating signs of $c_{a,i}$ and $c_{b,j}$. It is plausible that this matrix element is of the form $\surd qg(c_{a,i},c_{b,j})e^{-2Rab/\xi}$ and the preexponential factor g is only a weak function of R_{ab}/ξ for $R_{ab}/\xi<1$. Obtaining the orthogonalized localized states ψ_a and ψ_b for a random distribution of donors for $0.95n_c<n<0.99n_c$ is a difficult computation well beyond the scope of this work. However, the experimental fact that s is very small in the critical regime suggests the matrix element $\langle\psi_b|e^{i\mathbf{q}\cdot\mathbf{r}}|\psi_a\rangle$ does not depend much on R_{ab}/ξ, except for the envelope factor $e^{-Rab/\xi}$, thus leading to a T dependence of Mott VRH arising only from the exponential dependence $\exp-(T_0/T)^{1/4}$. It has been argued[39] for the case $T_0/T<1$ one cannot separate the prefactor T dependence from that in the exponential. The LD approach, as used by SKC and Delehaye, Brison, and Berger[41] in the low-T regime where $\sigma_t\sim\sigma_h$, allows one to separate the prefactor and exponential T dependences.

The above results for the 7.90 and 8.41 samples exhibit a good fit to the Mott law with $s-0$ up to temperatures above

or well above the Mott T_0 determined from the data for 0.5 $<T<5$ K. The Mott hopping energy $\Delta_h=1/4(T^3T_0)^{1/4}$ at $T_{\max}$ shown in Table I is still well below $E_{a,c}$. Furthermore, the ratio $\Delta_h/E_{a,c}$ is decreasing as $n\rightarrow n_{c-}$. In addition, even though the values of R_h/ξ are less than 1, the values of R_h are safely above the mean donor spacing d because of the large increase in $\xi(n)$ as $n\rightarrow n_{c\text{-}}$. R_h/ξ varies between 0.86 and 0.38 as T increases from 0.5 K to $T_{\max}$ for the 7.90 sample while R_h decreases from 164 to 71.6 Å for $\xi(7.90)=191$ Å with the mean donor spacing $d=50$ Å [for a Poisson distribution the most probable *nn* distance is $0.55d$]. The number of states in the hopping energy Δ_h range and mean hopping volume for Mott VRH is $N(E_F)[4\pi R_h^3/3]\Delta_h\sim 1$. This result is independent of magnitude of T_0/T and is valid for $R_h/\xi<1$ and $R_h/\xi>1$. The number of donor sites in a mean hopping volume is $(4\pi n/3)R_h^3=N_{D,hv}(n,T)\gg 1$. The result $(4\pi n/3)R_h^3\gg 1$ is an essential feature of Mott VRH and is satisfied over the entire range $0<T<77$ K for all four samples discussed above (and also for more dilute samples where $N_{D,hv}$ is even larger). For the 8.41 case $N_{D,hv}\sim 67$ at 1 K, 38 at 10 K, and 23 at 77 K. This leads directly to $\Delta_h=n/(N(E_F)N_{D,hv}\ll n/N(E_F)\sim 7$ meV for $N(E_F)\sim N(E_c)$ (see Table II). $\Delta_h(8.41,1\text{ K})\sim 0.013$ meV and $\Delta_h(8.41,77\text{ K})\sim 0.34$ meV. This inequality, using $R_h=3/8\xi(T_0/T)^{1/4}$, can also be rewritten as $R_h/\xi\ll 10.6n/N(E_F)kT$. This is satisfied for both $R_h/\xi>1$ at low T and for $R_h/\xi<1$ at high T. The notion that one does not have Mott VRH when $R_h/\xi<1$ is not supported by the experimental results, or by simple theoretical notions. The most important correction for Mott VRH prefactor for $T/T_0>2$ is the factor $n_h(T)/n=1-f_a$ discussed above. Of course, the Mott VRH form of $\sigma(T,n<n_c)$ does not survive as $T\rightarrow 0$, however for $1-n/n_c<0.02$ one cannot get cold enough to observe the deviations from Mott VRH.

In summary, the LD approach has permitted the deconvolution of Mott VRH and activated hopping conduction in a region where both are important. A simple high-temperature correction to Mott VRH has improved the determination of the activation energies and the temperature-dependent prefactor exponents of $\sigma_{a,c}(T)$. T-dependent activation energies are obtained for the two samples closest to n_c, possibly resulting from T-dependent changes in the chemical potential. This work illustrates the problems of evaluating activation energies from the slope of $\ln\rho(T)$ vs $1/T$ plots and suggests careful studies of transport using the LD approach may yield new and useful information on the DOS in the region just above the mobility edge. The fraction $f_a(n,T)$ of thermally activated itinerant electrons has been obtained with a theoretical expression, but can also be determined directly using the LD expressions and the experimental data. The deconvolution determining $\sigma_{a,c}(n,T)$ and $f_a(n,T)$ permits the direct determination of the mobility $\mu_{a,c}(n,T)$ of itinerant electrons in the donor impurity band. The results for $\mu_{a,c}(n,T)$ are in approximate agreement with Conwell-Weisskopf theory, although the two samples closest to n_c exhibit nearly T-independent $\mu_{a,c}(n)$ values at intermediate T that are qualitatively consistent with the modified Conwell-Weisskopf theory.

ACKNOWLEDGMENT

This work was supported in part by the National Science Foundation Grant No. DMR-83-06106.

APPENDIX A: THE TEMPERATURE DEPENDENT $\mu(T)$

Using Eq. (6) and the Sommerfeld expansion approach and the fact that $f(1-f)=-(\partial f/\partial E)T$ is an even function about $\mu(T)$ with the property $\int_{-\infty}^{+\infty}-(\partial f/\partial E)dE=1$ one obtains

$$d\delta\mu/dT=-\frac{[2a_1T(dN/dE)_\mu+4a_2T^3(d^3N/dE^3)_\mu+6a_3T^5(d^5N/dE^5)_\mu+\cdots+3n_{\mathrm{CB}}(T)/2]}{[N(\mu)+a_1T^2(d^2N/dE^2)_\mu+a_2T^4(d^4N/dE^4)_\mu+a_3T^6(d^6N/dE^6)_\mu+\cdots+n_{\mathrm{CB}}(T)]},\quad\text{(A1)}$$

where $a_1=\pi^2/6=1.6449$, $a_2=7\pi^4/360=1.894$, and $a_3=(31/16)\pi^6/945=1.9711$. The contribution $n_{\mathrm{CB}}(T)=C_eT^{3/2}e^{-(Ecb-\mu(T))/T}$ results from the Si conduction band and has been calculated with $f(1-f)\sim e^{-[E-\mu(T)]}\ll 1$ for the T range of the the experimental data. All of the derivatives d^pN/dE^p are calculated from the impurity band DOS in Fig. 1 with an interval $\Delta E=0.1$ meV and are evaluated at $\mu(T)$. Unlike the case for good metals the more rapid variation of the DOS(E) with E requires the evaluation of much higher derivatives for $p=5$ and 6 because of their importance at higher temperatures. If $N(E)$ were perfectly symmetrical about some energy E^* and at $T=0$ $\mu(0)=E_F=E^*$ then $d\mu(T)/dT=0$. The best results were obtained using a clamped spline interpolation. Since there was some scatter in dN^4/dE^4 near the end points the range was made large enough to be at least 8 meV above and below E_F. Based on a fit $N(E)=N(E_m)+\Sigma_2^6B_p(E-E_m)^p$ the B_p were obtained from the numerically determined derivatives. As expected from Fig. 1 showing an asymmetry about E_m B_3 is positive, while B_4 is negative since the quadratic behavior away from E_m is reduced further away from E_m. From the energy dependence of dN^4/dE^4 one can determine B_5 and B_6. B_6 is positive and counters the negative contribution from dN^4/dE^4 in the denominator in Eq. (A1). At larger T, dN^3/dE^3 drives $\mu(T)$ negative. Initially dN^5/dE^5 is positive and also aids in driving $\mu(T)$ down, but for $T\sim 2.75$ meV dN^5/dE^5 changes sign and opposes dN^3/dE^3. The problem with the Sommerfeld expansion is the slow convergence of both numerator and denominator because of important contributions from the higher derivatives.

TABLE III. Correction factor $(\alpha^2/384)(k^2 T_o T/16)$ at $T = 78$ K.

α	7.39	7.57	7.90	8.41
0.1 meV^{-1}	1.4×10^{-3}	2.6×10^{-4}	1.3×10^{-5}	1.3×10^{-7}
0.5 meV^{-1}	3.4×10^{-2}	6.5×10^{-3}	3.2×10^{-4}	3.2×10^{-6}

APPENDIX B: CORRECTION TO MOTT VRH FROM VARIATION IN THE DOS

In the exponential of the Mott VRH expression the Mott temperature $T_0 \propto 1/N(E_F)$. When the DOS $N(E)$ is varying in the vicinity of E_F there will be a correction of the form

$$(1/\Delta_h)\int_{\mu(T)-\Delta h/2}^{\mu(T)+\Delta h/2} \exp-[T_o N(\mu)/TN(E)]^{1/4} \quad dE, \tag{B1}$$

where $\Delta_h = 1/4(T^3 T_0)^{1/4}$ is the Mott hopping energy. Only the DOS variation in an energy range of order Δ_h about $\mu(T)$ is important. Employing a Taylor series expansion about $\mu(T)$ one has $[N(\mu)/N(E)]^{1/4} = 1 - 1/4\alpha(\mu)(E-\mu) + \text{h.o.}$, where $\alpha(\mu) = d\ln N(E)/dE_\mu$. Inserting in (B1) one finds

$$(1/\Delta_h)\exp-(T_o/T)^{1/4}\int_{-\Delta h/2}^{\Delta h/2} e^{a\epsilon} d\epsilon$$
$$= \exp-(T_o/T)^{1/4}[1 + a^2\Delta_h^2/24 + \cdots], \tag{B2}$$

where $a = (\alpha/4)(T_0/T)^{1/4}$. Inserting Δ_h into this result the leading correction term is given as $(\alpha^2/384)(k^2 T_0 T/16)$. The magnitude of this correction is given in Table III and is small. If the expression (B1) is averaged over $2\Delta_h$ rather than Δ_h, the correction factor increases by a factor of 4. This correction is given in Table III for two different values of $\alpha = d\ln N(E)/dE|_{\mu(T)}$. For the DOS in Fig. 1 typical values of $|\alpha|$ are of order 0.05 to 0.1 in the vicinity of $\mu(T)$. The correction in Mott VRH due to DOS variations is very small near n_c because T_0 scales to zero as $(1-n/n_c)^{3\nu}$ with $3\nu \sim 2.5 \pm 0.5$. With $\Delta_h \propto (T^3 T_0)^{1/4} \propto T^{3/4}(1-n/n_c)^{3\nu/4}$ this explains why this correction is negligible for n approaching n_c.

APPENDIX C: MODIFIED MANSFIELD (Ref. 31) EXPRESSIONS FOR THE IMPURITY BAND CASE

Mansfield's general expression [his Eq. (3)] for the conductivity of itinerant electrons in the conduction band (CB) resulting from ionized impurity scattering is

$$\sigma_I = [32\epsilon^2 m^*(kT)^3/3N_I e^2 h^3]$$
$$\times \int_0^\infty \eta^3 e^{\eta-\eta^*}/[(e^{\eta-\eta^*}+1)^2 f(x)]d\eta, \tag{C1}$$

where $\eta = E/kT$, $\eta^* = \mu(T)/kT$, and $f = [e^{\eta-\eta^*}+1]^{-1}$. For the CB $N(E) \propto (E-E_{CB})^{1/2}$ while for the impurity band for $E > E_c$ $N(E) = N(E_c)[1 + \alpha(T)(E-E_c) + \cdots]$. The data and analysis suggest $q \sim 1$ at higher T suggesting $\alpha(T)$ is small at higher T, probably resulting from $E_c(T)$ being near the minimum in $N(E)$. Multiplying Eq. (C1) by $N(E_c)h^3/[4\pi(2m^*)^{3/2}(E-E_{CB})^{1/2}]$ yields

$$\sigma_I = [8\epsilon^2 N(E_c)/3e^2 h N_I](\hbar kT/2m^*)^{1/2}(kT)^2$$
$$\times \int_0^\infty \eta^{5/2} f(1-f)/f(X)d\eta. \tag{C2}$$

The traditional approximation made removes $f(X) = \ln(1+X)$ from the integrand based on the notion $f(X)$ is slowly varying. $f(X)$ is then evaluated using $n \sim 3$ since this is the value of η where the integrand in (C1) is a maximum. However, this is not valid for values of $X \ll 1$ since in this case $f(X)$ is rapidly varying and approaches zero as $X \to 0$. Substituting $X = [\epsilon\eta kT/e^2 N_1]^2$ for the regime $f(X) \sim X \ll 1$ (C2) becomes

$$\sigma_I = [8N(E_c)/3N_I^{1/3}](e^2/h)(\hbar^2 kT/2m^*)^{1/2}$$
$$\times \int_0^\infty \eta^{1/2} f(1-f)d\eta. \tag{C3}$$

The strong dependence of $f(X)$ on X and η for small values of η permits low-energy scattering to be properly taken into account, whereas the assumption $f(X)$ is slowly varying underestimates the low-energy scattering. A better procedure breaks the integral in (C2) into two parts, namely, $\int_0^{\eta c}$ and $\int_{\eta c}^\infty$ with η_c determined by $\sqrt{X_c} = [\epsilon\eta_c kT/e^2 N_I^{1/3}] = 1$. This gives two terms with different temperature dependences. Integrating (C3) by parts yields $F_{-1/2}(\eta^*) = \int_0^\infty \eta^{-1/2} f d\eta$ producing Eq. (10).

An alternative approach for obtaining σ_I that avoids the $f(X)$ function in (C1) makes use of the collision rate $1/\tau$ determined from the phase shifts and the Friedel sum rule restriction for the semiconductor impurity band case,[30] namely,

$$Z(\pi/2) = (kT)^{-1}\Sigma_l(2l+1)\int_0^\infty \delta_l(E) f(1-f)dE. \tag{C4}$$

The scattering rate[30] $1/\tau = N_I v\langle\sigma\rangle = 4\pi N_I(\hbar/m^*k)\Sigma_l(l+1)\sin^2(\delta_l - \delta_{l+1})$ where the phase shifts δ_l depend on both temperature and energy and, using the relation $\delta_l \propto (ka)^{2l+2}$, are of the form $\delta_l(\eta,T) = a_l \eta^{l+1}/F_l(\eta^*)(l+1)$. The Fermi integral $F_l(\eta^*) = \int_0^\infty \eta^l (e^{\eta-\eta^*}+1)^{-1} d\eta$ and the Friedel sum rule yields $\Sigma_l(2l+1)a_l = \pi/2$ for $Z = 1$. Following the above procedure modifying the DOS to $N(E_c)$, but starting with Mansfield's Eq. (1) containing τ, the expression for $\sigma_{I,ps}$ for the impurity band is

$$\sigma_{I,ps} = (e^2/2h)[kTN(E_c)/N_I]$$
$$\times (2m^*kT/\hbar^2)^{1/2}\int_0^\infty \frac{\eta^{3/2} f(1-f)d\eta}{\Sigma_l(l+1)\sin^2(\delta_l - \delta_{l+1})}. \tag{C5}$$

The prefactor in (C5) differs from that in (C3) with different dependences on T, N_I, and m^*. For a given set of phase shifts $\delta_l(\eta,T)$ the integral in (C5) can be evaluated, but it must be evaluated for each T of interest.

*Present address: Institute of Energy Conversion, University of Delaware, Newark, DE 19716.

[1] H. Fritzsche, Phys. Rev. **99**, 406 (1955).
[2] A. Miller and E. Abrahams, Phys. Rev. **120**, 745 (1960).
[3] N. F. Mott, J. Non-Cryst. Solids **1**, 1 (1969).
[4] F. R. Allen and C. J. Adkins, Philos. Mag. **20**, 1027 (1972).
[5] A. L. Efros and B. I. Shklovskii, J. Phys. C **8**, L49 (1975).
[6] G. Biskupski, H. Dubois, and A. Briggs, J. Phys. C **21**, 333 (1988).
[7] Y. Zhang, P. Dai, M. Levy, and M. P. Sarachik, Phys. Rev. Lett. **64**, 2687 (1990).
[8] R. Rosenbaum, Phys. Rev. B **44**, 3599 (1991).
[9] I. Shlimak, M. Kaveh, M. Yosefin, M. Lea, and P. Fozooni, Phys. Rev. Lett. **68**, 3076 (1992).
[10] A. Aharony, Y. Zhang, and M. P. Sarachik, Phys. Rev. Lett. **68**, 3900 (1992).
[11] R. Rosenbaum, N. V. Lien, M. R. Graham, and M. Witcomb, J. Phys.: Condens. Matter **9**, 6427 (1997).
[12] B. I. Shklovskii, Fiz. Tekh. Poluprovdn. **6**, 1197 (1972) [Sov. Phys. Semicond. **6**, 1053 (1973)].
[13] W. N. Shafarman, D. W. Koon, and T. G. Castner, Phys. Rev. B **40**, 1216 (1989); W. N. Shafarman and T. G. Castner, *ibid.* **33**, 3570 (1986).
[14] R. N. Hill, Phys. Status Solidi A **35**, K29 (1976).
[15] M. Levy, A. Roy, M. P. Sarachik, and L. L. Isaacs, Phys. Rev. B **38**, 3323 (1988).
[16] A. G. Zabrodskii, A. G. Andreev, and M. V. Alekseenko, Fiz. Tekh. Poluprovodn. **26**, 431 (1992) [Sov. Phys. Semicond. **26**, 244 (1992)]; A. G. Zabrodskii and A. G. Andreev, Int. J. Mod. Phys. B **8**, 883 (1994).
[17] J. G. Massey and M. Lee, Phys. Rev. Lett. **75**, 4266 (1995); **77**, 3399 (1996).
[18] A. Moebius, J. Phys. C **19**, L49 (1975); J. Non-Cryst. Solids **97&98**, 225 (1987); J. Phys. C **21**, 2789 (1988); Phys. Rev. B **40**, 4194 (1989); Solid State Commun. **73**, 215 (1990).
[19] A. Moebius, H. Vinzelberg, C. Gladun, A. Heinrich, D. Elefant, J. Schumann, and G. Zies, J. Phys. C **18**, 3337 (1985).
[20] F. Stern, Phys. Rev. B **9**, 4597 (1974).
[21] R. L. Aggarwal and A. K. Ramdas, Phys. Rev. **140**, 1246 (1965).
[22] T. G. Castner, Phys. Rev. B **21**, 3523 (1980).
[23] R. A. Smith, *Semiconductors* (Cambridge, London, 1968), p. 91.
[24] E. Conwell and V. F. Weisskopf, Phys. Rev. **77**, 388 (1950).
[25] W. Shockley, *Electrons and Holes in Semiconductors* (Van Nostrand, New York, 1950), p. 288.
[26] H. Brooks, in *Advances in Electronics and Electron Physics*, edited by L. Marton (Academic, New York, 1955), Vol. 7, p. 85.
[27] N. Takimoto, J. Phys. Soc. Jpn. **14**, 1142 (1959).
[28] D. Chattopadhyay and H. J. Queisser, Rev. Mod. Phys. **53**, 745 (1981).
[29] C. Yamanouchi, K. Miziguchi, and W. Sazaki, J. Phys. Soc. Jpn. **22**, 859 (1967).
[30] B. A. Sanborn, P. B. Allen, and G. D. Mahan, Phys. Rev. B **46**, 15 123 (1992).
[31] R. Mansfield, Proc. R. Soc. London, Ser. B **69**, 76 (1956).
[32] M. Grunewald, H. Mueller, P. Thomas, and D. Wuertz, Solid State Commun. **38**, 1011 (1981).
[33] D. W. Koon and T. G. Castner, Solid State Commun. **64**, 11 (1987).
[34] D. W. Koon and T. G. Castner, Phys. Rev. B **41**, 12 054 (1990).
[35] F. J. Blatt, J. Phys. Chem. Solids **1**, 262 (1957).
[36] P. F. Newman, M. J. Hirsch, and D. F. Holcomb, J. Appl. Phys. **58**, 3779 (1985).
[37] J. A. del Alamo and R. M. Swanson, J. Appl. Phys. **57**, 2314 (1985).
[38] C. Erginsoy, Phys. Rev. **79**, 1013 (1950).
[39] P. Dai, S. Bogdanovich, Y. Zhang, and M. S. Sarachik, Phys. Rev. B **52**, 12 439 (1995).
[40] H. Stupp, M. Hornung, M. Lakner, O. Madel, and H. v. Löhneysen, Phys. Rev. Lett. **71**, 2634 (1993); comment, T. G. Castner, *ibid.* **73**, 3600 (1994).
[41] J. Delahaye, J. P. Brison, and C. Berger, Phys. Rev. Lett. **81**, 4204 (1998).
[42] T. G. Castner, in *Hopping Transport in Solids*, edited by M. Pollak and B. Shklovskii (Elsevier Science, New York, 1991), p. 8.